

Worcester Polytechnic Institute Digital WPI

Major Qualifying Projects (All Years)

Major Qualifying Projects

April 2011

Biofuels from Microalgae: A Study of Growth Conditions in *Ettlia oleoabundans*

Andrea Rose Tarbet

Worcester Polytechnic Institute

Benjamin Gustav Mininberg

Worcester Polytechnic Institute

Follow this and additional works at: <https://digitalcommons.wpi.edu/mqp-all>

Repository Citation

Tarbet, A. R., & Mininberg, B. G. (2011). *Biofuels from Microalgae: A Study of Growth Conditions in Ettlia oleoabundans*. Retrieved from <https://digitalcommons.wpi.edu/mqp-all/333>

This Unrestricted is brought to you for free and open access by the Major Qualifying Projects at Digital WPI. It has been accepted for inclusion in Major Qualifying Projects (All Years) by an authorized administrator of Digital WPI. For more information, please contact digitalwpi@wpi.edu.

Biofuels from Algae: A Study of Growth Conditions in *Ettlia oleoabundans*

A Major Qualifying Project Report
submitted to the Faculty
of
WORCESTER POLYTECHNIC INSTITUTE
in partial fulfillment of the requirements
for the Degree of Bachelor of Science



By

Andrea R. Tarbet

Benjamin Mininberg

Approved by:

Dr. Pamela J. Weathers

April 28, 2011

Abstract

Biofuels derived from algae can provide a source of renewable fuel and facilitate the break from fossil fuel dependency. Algae produce triacylglycerols (TAGs), which can be cost effectively converted into biofuel. Light intensity and temperature affect growth and oil production of algae. *Ettlia oleoabundans*, an algal species that produces >50% of its weight as TAGs, grew and produced oils at 15 and 25 °C and light intensities under 200 $\mu\text{mol m}^{-2} \text{sec}^{-1}$, conditions common to New England. Optimizing growth conditions will help in the development of efficient and economical biofuel production.

Contents (indicates authorship)

Abstract.....	2
Table of Figures.....	5
Table of Tables	6
Acknowledgements.....	7
Chapter 1: Introduction and Background (AT).....	8
1.1 Benefits of Biofuels (BM)	8
1.1.1 Human Health Benefits (BM)	8
1.1.2 Environmental Benefits (BM)	9
1.1.3 Economic Benefits (BM)	10
1.2 Microalgae as a Biofuel Source (AT).....	11
1.2.1 Microalgae Growth Requirements (AT).....	11
1.2.2 Issues with Controlling Mass Cultures of Algae (AT).....	11
1.2.3 Biochemistry of Triacylglycerol Microalgae (AT)	12
1.3 Biofuel Production and Quality (AT).....	16
1.3.1 Transesterification (AT)	16
1.3.2 Future Technologies (AT)	17
1.3.3 Biofuel Quality (AT).....	18
1.4 An Algal Candidate for Biofuel Production: <i>Ettlia oleoabundans</i> (BM).....	18
1.4.1 <i>Ettlia oleoabundans</i> (BM)	19
1.5 Growth Parameters	21
1.5.1 Light Intensity (AT).....	22
1.5.1.1 <i>Algae and the Light Reactions of Photosynthesis</i>	22
1.5.1.2 <i>Algae and the Calvin-Benson Cycle of Photosynthesis</i>	22
1.5.1.3 <i>Regulation of Photosynthesis</i>	23
1.5.1.4 <i>Function of Light Intensity</i>	24
1.5.1.5 <i>Light Availability</i>	24
1.5.1.6 <i>Past Studies</i>	26
1.5.2 Temperature (BM)	28
Chapter 2: Hypotheses and Objectives (AT, BM).....	29
Chapter 3: Methods	29
3.1 Maintenance of Stock Cultures (AT, BM).....	29
3.2 Light Intensity and Temperature (AT, BM)	29
3.3. Growth Analysis (AT, BM)	30

3.4 Oil Concentration (AT, BM)	31
3.5 Gravimetric Analysis (AT, BM)	31
3.6 End Media Analysis (AT, BM)	31
3.7 Gas Chromatography-Mass Spectrometry (AT, BM)	31
3.8 Statistical Analysis (AT, BM)	32
Chapter 4: Results (AT, BM)	32
4.1 Growth of <i>Ettlia</i> at 4 temperatures and 3 light intensities.	32
4.2 Oil Detection and Analysis	35
4.3 Oil Composition	38
Chapter 5: Discussion (AT, BM)	41
Chapter 6: Conclusions and Future Research	44
References	46
Appendix A	50
Appendix B	51
Appendix B Continued	52
Appendix C	53
Appendix D	54
Appendix E	55
Appendix F	56

Table of Figures

Figure 1: World oil production versus world oil discovery (taken from Day <i>et al.</i> , 2009).....	8
Figure 2: Worldwide commodity prices compared to the cost of crude oil per barrel from 1990-2008 (taken from Senauer, 2008).	11
Figure 3: Lipid synthesis in plant plastids (taken from Taiz and Zeiger, 2010).....	13
Figure 4: The Kennedy pathway adds three lipids per glycerol molecule, forming a TAG (taken from Lung and Weselake, 2006).	14
Figure 5: Glycerol molecule which forms the backbone of a TAG (taken from Monash Scientific, 2000).	14
Figure 6: Triacylglycerols are produced in plants and similarly in algae, and are used for biodiesel production (taken from Taiz and Zeiger, 2010).	15
Figure 7: Oil bodies formed in plants store TAGs (taken from Taiz and Zeiger, 2010).....	15
Figure 8: Transesterification process for transforming bio oil into biodiesel (taken from Taiz and Zeiger, 2010).	17
Figure 9: Microalgae <i>E. oleoabundans</i> (taken from UTEX, 2010).	20
Figure 10: <i>E. oleoabundans</i> confocal fluorescence microscope image.....	20
Figure 11: Regulation of the carbon reactions of photosynthesis by light and supramolecular complexes (taken from Taiz and Zeiger, 2010).	23
Figure 12: The Effects of CO ₂ on photosynthesis (taken from Taiz and Zeiger, 2010).....	26
Figure 13: Experimental setup. Light intensities are measured in $\mu\text{mol m}^{-2} \text{sec}^{-1}$	30
Figure 14: Average cell dry weights (g/L) of <i>E. oleoabundans</i> grown at 15°C, 25°C; and 35°C for 70 (triangles), 130 (squares), and 200 (circles) $\mu\text{mol m}^{-2} \text{sec}^{-1}$	34
Figure 15: Flask A from each light intensity at 35°C at day seven, demonstrating changes in culture color.	35
Figure 16: Average Nile red fluorescence readings of <i>E. oleoabundans</i> grown under 15°C, 25°C, and 35°C for 70 (triangles), 130 (squares), and 200 (circles) $\mu\text{mol m}^{-2} \text{sec}^{-1}$	37
Figure 17: Average annual temperatures of Portugal (taken from Climate Charts, 2010).	42
Figure 18: Average annual temperatures of Worcester, MA, a city in Northeastern US (taken from Climate-Charts, 2010).....	45

Table of Tables

Table 1: Motor vehicle emissions and their human health effects (taken from Liaquat et al., 2010) ..	9
Table 2: Nitrogen and phosphorus levels decrease in wastewater over time when supplied to algal cultures in two types of photobioreactors (PBR) (taken from Kong <i>et al.</i> , 2009).....	12
Table 3: Comparison of oil production and land requirements between various crops considered for biodiesel production (taken from Schenk <i>et al.</i> , 2008).....	16
Table 4: How fuel properties are affected by fatty acid composition in a biofuel (taken from Knothe, 2005).	19
Table 5: Summary of cell growth, lipid production, and nitrogen consumption results obtained with media with different sodium nitrate (taken from Gouveia <i>et al.</i> , 2009).....	21
Table 6: Average photosynthetic photon flux (PPF) for healthy plant growth (taken from Apogee Instruments Inc., 2010).....	25
Table 7: Peak Average Dry Weights.....	35
Table 8: Biomass productivity and yield for each experimental run.....	35
Table 9: Nile red peak readings.....	38
Table 10: Comparison in peak % oil and extractives per algae.....	38
Table 11: GC-MS results for 15°C and 25°C presented as percent specific FAME per extractive.....	40
Table 12: GC-MS results for 15, 25, and 25°C presented as percent specific FAME per lipids.....	40
Table 13: Comparison to Gouveia and Oliveria (2008) results for <i>E. oleoabundans</i> for productivity and peak biomass.....	41
Table 14: Comparison to Gouveia (2009) results for <i>E. oleoabundans</i> for peak oil per algae.....	42

Acknowledgements

We would like to thank the following group of colleagues for aiding us in a year long journey, our Major Qualifying Project. First, our advisor, Professor Weathers, allowed us to work in this project in her lab and continually guided us through this vital aspect of our college careers. Ying Yang helped us develop our project, accomplish our goals, analyzed oil by GC-MS, and answered every question we could conjure. Melissa Towler, Khanhvan Nguyen, Liwen Fei, and Praphapan “Beer” Lasin helped us around the lab and gave us advice. Andrew Keyser and Juan Gomez shared space with us in the lab and gave us a few good laughs.

Andrea would also like to thank the following people who made this project possible. To my greatest supporter, Kevin McManus, for always being there for me and loving me no matter how stressed out I became this year. A great thanks to my parents provided me with the means and continual support to attend WPI which not all young adults my age receive and one day I’ll get you the pineapple plantation in Hawaii where you can retire.

Ben would also like to thank the following:

My parents for providing me the opportunity to work on such an important and challenging project.

Professor Crusberg and Victoria Hunter for helping me take the Confocal Fluorescence images.

Chapter 1: Introduction and Background (AT)

Since the 1950's, the global oil demand has increased from 11 million barrels per day (MBD) to a currently estimated 80 MBD (Wright, 2008). Although the exact year when the oil supply will be exhausted is unknown, economists predict that the oil production exceeds the oil deposit discovery rate (Figure 1). The world oil discovery rate peaked in the 1970's, and a quarter of the world's super oil fields have been declining in production each year since (Day *et al.*, 2009). The demand for oil has increased at an astounding rate due to the growing global population and countries becoming more industrialized. Finding sustainable and renewable energy resources for the planet is imperative for the survival of modern day society. Furthermore, if renewable energy can be generated locally, then less energy is lost during distribution. Microalgae can produce high amounts of fatty acids which can be converted into biodiesel and thus offer such a resource. This project focuses on how light intensity and temperature affect algal growth and oil yield of an oil forming algal species which is a possible key to finding a feasible and sustainable alternative liquid transportation fuel.

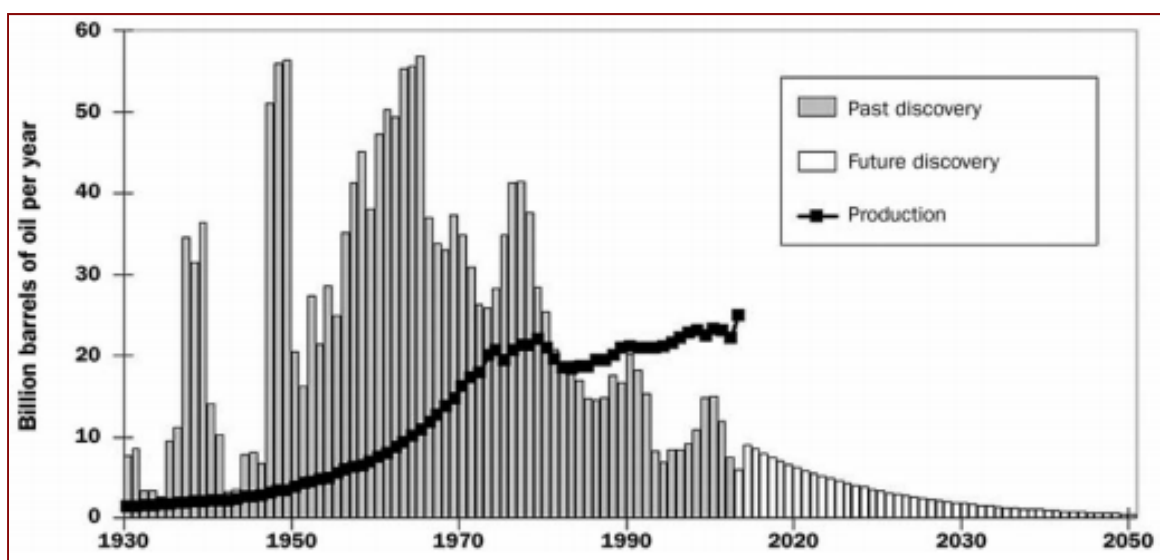


Figure 1: World oil production versus world oil discovery (taken from Day *et al.*, 2009).

1.1 Benefits of Biofuels (BM)

Biofuels, which are fuels derived from a biological feed stock, are an alternative energy source drawing great attention. Biofuels have many benefits, ranging from improved human health to an improved environment.

1.1.1 Human Health Benefits (BM)

Fuels combusted by automobiles represent a substantial source of many harmful air pollutants. These harmful compounds include carbon monoxide, mutagenic hydrocarbons, and carcinogenic aromatics (Table 1; Liaquat, *et al.*, 2010). Biofuels show significant

promise in reducing the pollution released by fossil fuels because they simply do not contain many of the harmful chemicals present in traditional fuels (Liaquat, *et al.*, 2010).

Table 1: Motor vehicle emissions and their human health effects (taken from Liaquat et al., 2010)

Exhaust emissions	Health Effects
Carbon Monoxide	Impairs perception and thinking, slows reflexes, causes drowsiness, brings on angina, and can cause unconsciousness and death; it affects fetal growth in pregnant women and tissue development of young children. It has a synergistic action with other pollutants to promote morbidity in people with respiratory or circulatory problems
Nitrogen Oxides (NO₂, NO₃)	Can increase susceptibility to viral infections such as influenza; irritate the lungs and cause edema, bronchitis and pneumonia; and result in increased sensitivity to dust and pollen in asthmatics. Most serious health effects are in combination with other air pollutants
Hydrocarbons and other Volatile Organic Compounds	Low-molecular weight compounds: Eye irritation, coughing and sneezing, drowsiness and symptoms akin to drunkenness. Heavy molecular weight compounds: may have carcinogenic or mutagenic effects. Some hydrocarbons have a close affinity for diesel particulates and may contribute to lung disease
Ozone (Precursors: HC & NO_x)	Causing coughing, choking, and impaired lung function; causes headaches and physical discomfort; reduces resistance to colds and pneumonia; can aggravate chronic heart disease, asthma, bronchitis, and emphysema
Lead	Affects circulatory, productivity nervous, and kidney systems suspected of causing hyperactivity and lowered learning ability in children; hazards even after exposure
Particulate Matter (PM)	Respiratory problems, lung cancer and cardiopulmonary deaths
Toxic Substances	Causing cancer, reproductive problems, and birth defects. Benzene and asbestos are known carcinogens; aldehydes and ketones irritate the eyes, cause short-term respiratory and skin irritation and may be carcinogenic
Polycyclic aromatic hydrocarbons (PAHs)	Lung cancer
Formaldehyde	Eye and nose irritation, coughing, nausea and shortness of breath. Occupational exposure is associated with risk of cancer
Dioxin	Long-term exposure: Impairment of the immune system, the developing nervous system, the endocrine system and reproductive functions

1.1.2 Environmental Benefits (BM)

The harmful emissions released by traditional fossil fuels in automobiles have many detrimental effects to the environment including lead poisoning in wildlife (Liaquat, *et al.*, 2010). It is essential to our continued survival to reduce these threats to global health and well-being. Bio-synthesized fuels contain significantly fewer harmful compounds such as lead, carbon monoxide, and nitrogen oxides because they are not present in biological processes that generate the compounds used for biofuel production. Biodiesel and ethanol are the current leading biofuels, and even in limited use have resulted in a significant

decrease in harmful emissions (Liaquat, *et al.*, 2010). An additional study done comparing emissions from biodiesel and regular diesel found a significant decrease in harmful carbon monoxide using biodiesel. Therefore, using algal biofuel as a liquid transportation fuel should drastically reduce the amount of pollution released into the environment (Carretto, *et al.*, 2004).

An extensive study of air pollution in the congested urban environments of India found a direct correlation between air pollutant levels resulting from fossil-fuel use and human sickness (Mukhopadhyaya, 2005). Particularly hazardous were nitrous-oxide and sulfoxide compounds. Of special concern are the statistics showing a correlation between asthma-related deaths and an increase of airborne pollutants over time (Mukhopadhyaya, 2005). Ailments that are most likely being directly caused by these pollutants include chronic bronchitis.

These results make a bold case for the need to reduce airborne pollutants, and a shift away from conventional fossil fuels is a way to achieve that goal. Although a complete conversion from fossil fuels to biofuels is a long-term goal, biofuels have already shown significant results in pollutant emission reduction by being blended into traditional diesel and gasoline fuels for automotive use (Liaquat, *et al.*, 2010). Blends of up to 20% biodiesel with petroleum diesel fuel release noticeably fewer fumes, less odor, and contain appreciably lower levels of harmful emissions (Liaquat, *et al.*, 2010).

1.1.3 Economic Benefits (BM)

Commercial scale production of biofuels is costly in today's economy; however, there are still some socio-economic benefits from producing biofuels (Rutz and Janssen, 2007). Biofuel production offers opportunities for small businesses in the exclusive oil industry and overall creation of new jobs. Furthermore, biofuels can provide supplemental income for farms growing biofuel feedstocks (Rutz and Janssen, 2007).

The cost of crude oil has been steadily rising for the last decade (Senauer, 2008). Since the global economy is heavily based on crude oil, when the price of a barrel of crude oil rises, so does the cost of other commodities (Figure 2). In recent years, the simple matter of supply and demand has led to dramatically increased costs for fuel as well as incredible price sensitivity to even the slightest potential to disruptions in supply flow. As discussed above, the use of fossil fuels also causes many health problems and these problems pose their own economic strain through healthcare costs, albeit with a potentially longer time to observe a major impact (Mukhopadhyaya, 2005).

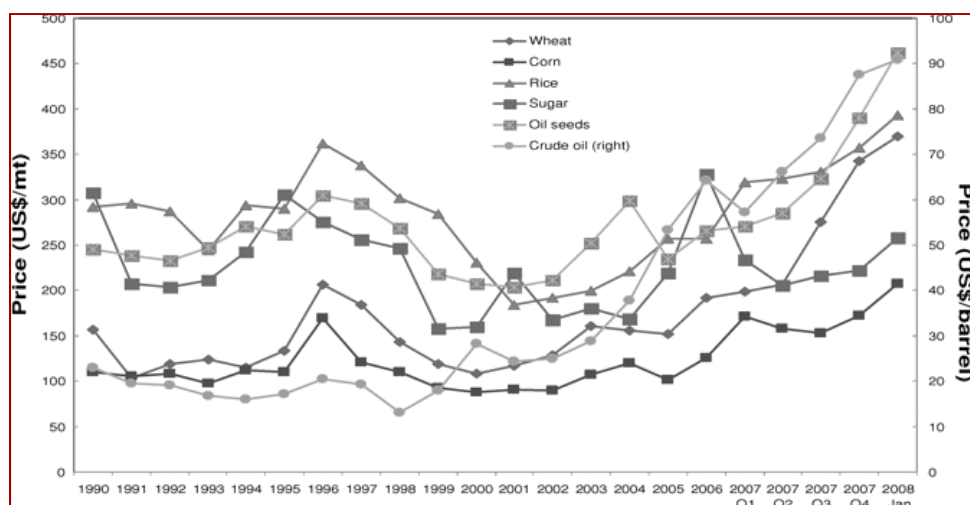


Figure 2: Worldwide commodity prices compared to the cost of crude oil per barrel from 1990-2008 (taken from Senauer, 2008).

1.2 Microalgae as a Biofuel Source (AT)

For an energy source to be considered as alternative and sustainable, it must be efficiently renewable and profitable. In other words, for biofuel to be successful, the biological feedstock must be able to grow quickly with few nutrient inputs, and the energy output of the fuel has to be far greater than the energy required for the entire lifecycle of the process. Most emphasis has been placed on using crops such as corn and soybeans for biofuel; however, there are issues surrounding using food crops as a fuel source. Using food crops as a biofuel resource competes with the food supply by devoting land to fuel instead of food. This is controversial because the competition may increase food prices of these crops, which can further strain economies. As a result, interest in using microalgae as a renewable energy source has been building momentum over recent years.

1.2.1 Microalgae Growth Requirements (AT)

Microalgae are relatively low maintenance organisms that require few nutrients to grow and thrive. Light, water, carbon dioxide, and inorganic nutrients such as nitrates, phosphates, iron and some trace elements are the only requirements for microalgae to grow and survive (Chisti, 2008). These nutrients provide microalgae with the materials to produce important compounds such as lipids and long chain hydrocarbons, which are the two basic molecules that can be converted to either biodiesel or cracked like petrol.

1.2.2 Issues with Controlling Mass Cultures of Algae (AT)

Although microalgae have few growth requirements, there are still problems cultivating microalgae on a scale large enough to produce biofuel to replace fossil fuels. As with any living organism, growing controlled mass cultures of microalgae requires a great amount of nutrients. Wastewater has become a promising source of nitrogen and phosphorus for mass cultures of algae. For example, Kong *et al.* (2009) showed that nitrogen and phosphorus levels from wastewater decrease over time in algal cultures,

suggesting the algae use these nutrients to grow and that they need an ample source of nutrition to grow faster (Table 2). Yang *et al.* (2011) showed that algae can grow and produce oil when supplied with effluents from anaerobically digested agricultural waste.

Table 2: Nitrogen and phosphorus levels decrease in wastewater over time when supplied to algal cultures in two types of photobioreactors (PBR) (taken from Kong *et al.*, 2009)

The types of PBR	Specific growth rate (day ⁻¹)	Cell concentration (cells mL ⁻¹)	N removal (mg L ⁻¹)	P removal (mg L ⁻¹)	Productivity (g L ⁻¹ day ⁻¹)	
					Biomass	Oil
Flasks	0.346±0.06	5.4×10 ⁷	40.36±0.04	15.08±0.02	0.82±0.04	0.136±0.01
			22.18±0.04	13.12±0.03		
Biocoil	0.564±0.05	7.6×10 ⁷	55.80±0.03	17.40±0.04	2.00±0.03	0.505±0.02

Additionally, the concentration of CO₂ affects photosynthesis in plants. When algae are provided with high levels of light and CO₂, photosynthesis increases, and when light intensity and CO₂ are low, photosynthesis decreases (Taiz and Zeiger, 2010). Mass culture of algae for fossil fuel replacement would require high concentrations of CO₂ to provide the carbon needed for lipid biosynthesis. Carbon dioxide capture is one method for providing mass cultures of algae with high and constant levels of CO₂. This method requires microalgae to be grown in either an open pond or a bioreactor system near sources of CO₂ such as coal fired power plants (Rasmussen, 2008). The algae in an open pond can naturally fix the CO₂ from the power plants as the gas is passed over the pond, but in a bioreactor, the gas is better controlled when captured and bubbled through the cultures (Rasmussen, 2008). With more research, it is possible to optimize nutrient feeds that can be used to grow algae thereby yielding the building blocks for biofuel.

1.2.3 Biochemistry of Triacylglycerol Microalgae (AT)

Different microalgae species can produce one of the two types of compounds, which can be used as sources for biodiesel: triacylglycerols (TAGs) and long chain hydrocarbons (LCH). A more in depth understanding of the biochemistry of TAGs and LCH is emerging from studies across the globe. This study focused on TAG production.

1.2.3.1 Biochemistry of Triacylglycerol Production (AT)

CO₂ is fixed into carbohydrates during the dark reactions of photosynthesis, and the energy is eventually stored inside microalgae in the form of lipids. Although the lipid biosynthetic pathway has not yet been completely determined for microalgal, research has shown that microalgae pathways are similar to plants (Taiz and Zeiger, 2010). The lipid biosynthetic pathway in plants occurs in the plant organelle, called the plastid (Figure 3).

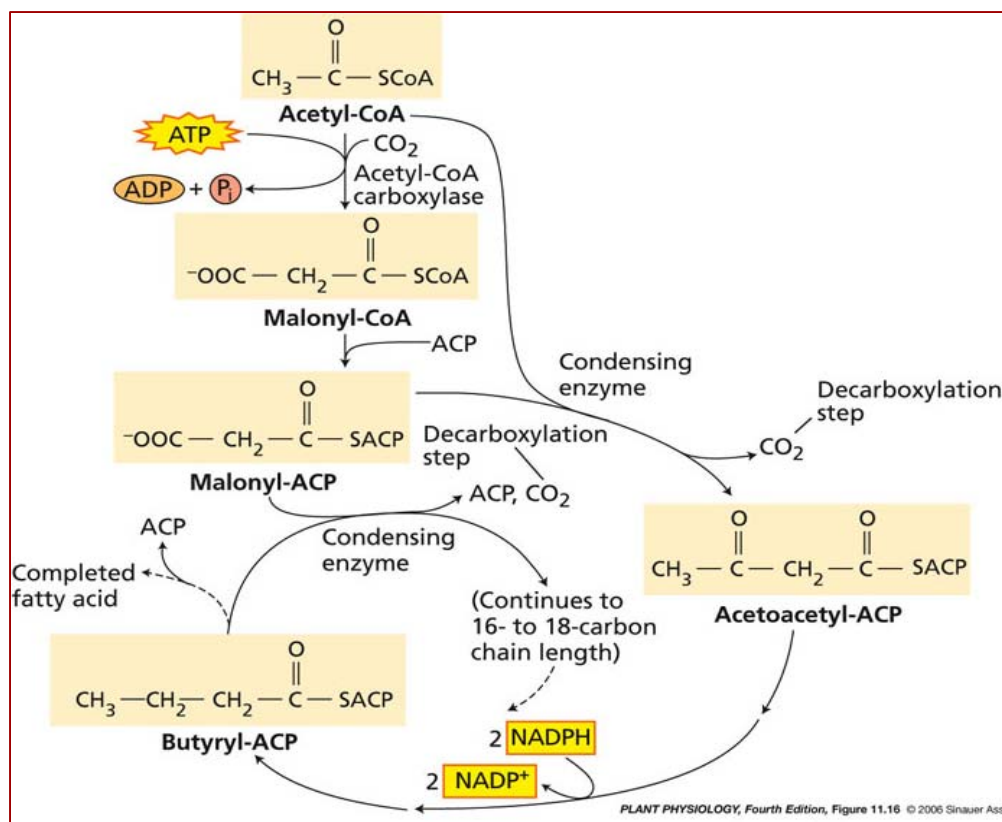


Figure 3: Lipid synthesis in plant plastids (taken from Taiz and Zeiger, 2010).

Biodiesel is not directly derived from the lipids produced in the pathway shown in plant plastids. Rather, the fatty acids undergo further modification in the plant cell endoplasmic reticulum (ER), resulting in TAGs, the precursor of biodiesel. The Kennedy Pathway (Figure 4) modifies lipids passing through the ER by linking the fatty acids to glycerol molecules (Figure 5) one at a time (Lung and Weselake, 2006). Three fatty acids are added per glycerol molecule, yielding a TAG (Figure 6).

The TAGs generated in the ER accumulate and break off as oil bodies (Figure 7). Oil bodies have single layered phospholipid membranes which keep the TAGs enclosed (Taiz and Zeiger, 2010). Membrane proteins called oleosins surround the oilbodies preventing them from interacting with one another by increasing their stability (Taiz and Zeiger, 2010). TAG accumulation and oil body formation in microalgae most likely follows the same biosynthesis in plants.

Many microalgal species accumulate high levels of TAGs during their stationary growth phase. The species *Ettlia oleoabundans* has been reported to produce up to 56% of its dry weight in TAGs (Gouveia *et al.*, 2009). Microalgae's ability to produce and store such high volumes of TAGs makes them prime candidates for a renewable energy source. Compared to other biological feedstocks such as soybeans and cotton, microalgae have

The diagram illustrates the following metabolic pathways:

- PLASTID:**
 - Acetyl-CoA is converted to malonyl-CoA by the enzyme ACCase.
 - malonyl-CoA is converted to malonyl-ACP.
 - malonyl-ACP enters the FAS (Fatty Acid Synthase) cycle to produce 16:0-ACP.
 - 16:0-ACP is converted to 18:0-ACP by the enzymes TS and ACS.
 - 18:0-ACP is converted to 18:1-ACP by the enzyme Δ^9 -DES.
- CYTOPLASM:**
 - 18:1-ACP is converted to 18:1-CoA.
 - 18:1-CoA enters the Acyl-CoA Pool.
 - 16:0-ACP and 18:0-ACP are converted to 16:0-CoA and 18:0-CoA, respectively, which also enter the Acyl-CoA Pool.
 - 18:0-CoA is converted to 18:1-CoA by the enzyme Δ^9 -DES.
 - 18:1-CoA is converted to 22:1-CoA by the enzyme FAE (Fatty Acid Elongase).
 - 18:1-CoA and 22:1-CoA are interconvertible.
- ENDOPLASMIC RETICULUM:**
 - G3P is converted to LPA by GPAT, using CoA.
 - LPA is converted to PA by LPAAT, using CoA.
 - PA is converted to DAG by PAP, releasing Pi.
 - DAG is converted to TAG by DGAT, using CoA.
 - DAG is converted to PC by CPT.
 - PC is converted to LPC by PLA₂.
 - LPC is converted to PC by LPCAT, using CoA.
 - DAG and TAG are interconvertible by DGTA and PDAT.
 - PC and LPC are interconvertible by PLA₂ and LPCAT.

$$\begin{array}{ccccccc} & \text{H} & & \text{H} & & \text{H} & \\ & | & & | & & | & \\ \text{H} & - \text{C} & - & \text{C} & - & \text{C} & - \text{H} \\ & | & & | & & | & \\ & \text{OH} & & \text{OH} & & \text{OH} & \end{array}$$

Glycerol

(Glycerine - propane 1,2,3, triol
- 3 hydroxyl (OH) functional group)

14

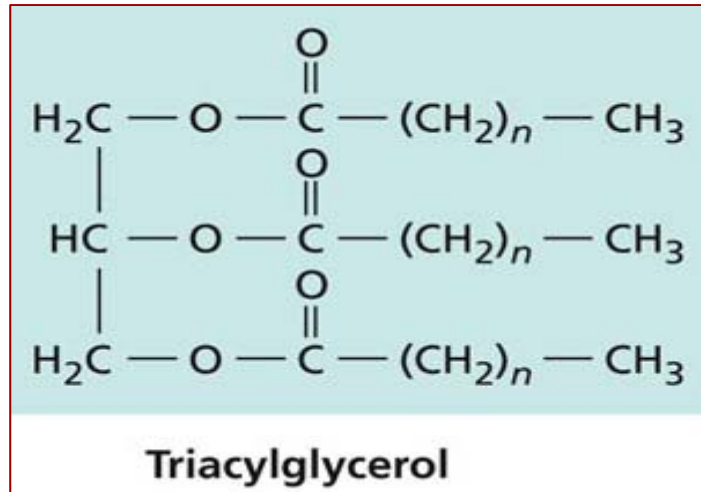


Figure 6: Triacylglycerols are produced in plants and similarly in algae, and are used for biodiesel production (taken from Taiz and Zeiger, 2010).

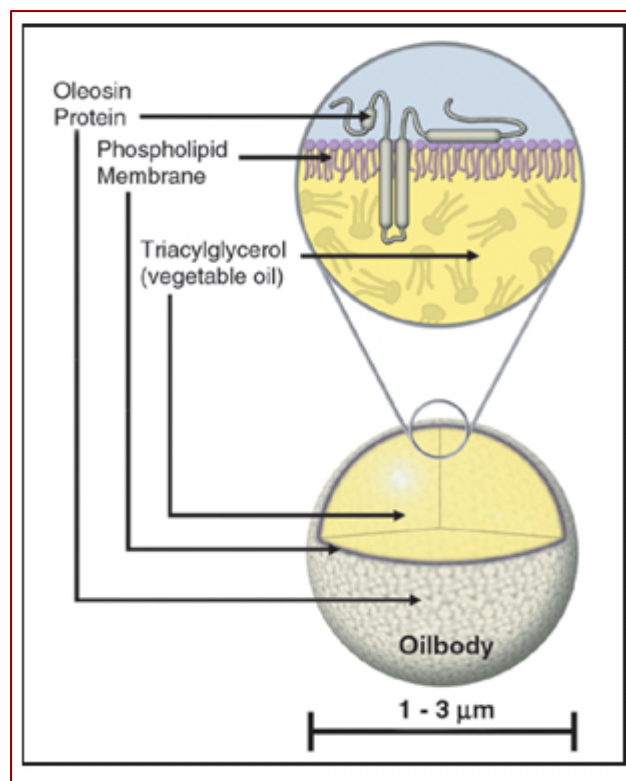


Figure 7: Oil bodies formed in plants store TAGs (taken from Taiz and Zeiger, 2010).

Table 3: Comparison of oil production and land requirements between various crops considered for biodiesel production (taken from Schenk *et al.*, 2008).

Plant Source	Biodiesel (L/ha/year)	Area to Produce global oil demand (hectares x 10 ⁶)	Area required as percent global land mass	Area as percent global arable land
Cotton	325	15, 002	100.7	756.9
Soybean	446	10, 932	73.4	551.6
Mustard Seed	572	8,524	57.2	430.1
Sunflower	952	5,121	34.4	258.4
Rapeseed/Canola	1,190	7,097	27.5	206.7
Jatropha	1,892	2,577	17.3	130
Oil Palm	5,950	819	5.5	41.3
Algae (10m ² day ⁻¹ at 30% TAG)	12,000	406	2.7	20.5
Algae (10m ² day ⁻¹ at 50% TAG)	98,500	49	0.3	2.5

1.3 Biofuel Production and Quality (AT)

TAGs produced by microalgae need to be extracted and converted into biofuel. In order for an energy source to be considered sustainable and efficient, the energy inputs must be lower than the energy outputs during the production process. One method currently dominates the microalgae oil conversion process, transesterification. Other processes, which hope to lower the energy inputs, are currently under experimentation. Furthermore, the quality of the biofuel also affects how successful a fuel will be in the market.

1.3.1 Transesterification (AT)

Oils that some species of algae produce are too viscous to be used as direct sources for biodiesel. The process known as transesterification converts algal oil into the constituent fatty acids, increasing fluidity and forming biodiesel, which can be used in engines (Figure 8; Scragg *et al.*, 2001). It may even be possible to use as fuel algae directly

mixed with petrol diesel as Scragg *et al.* (2001) has demonstrated. During transesterification, the lipids in the bio-oil react with an alcohol such as methanol to produce biodiesel and the by product, glycerol. This process requires low energy inputs, a temperature of 65.5°C and a pressure of 20psi (National Biodiesel Board, 2010). Furthermore, the by-product, glycerol, is used in beauty products such as soaps and lotions which currently off sets the cost of biodiesel production; however, if biodiesel becomes a majority commodity, then glycerol production will be excessive and the price will decline (Pachauri and He, 2006). Technology for efficient glycerol use will then be required.

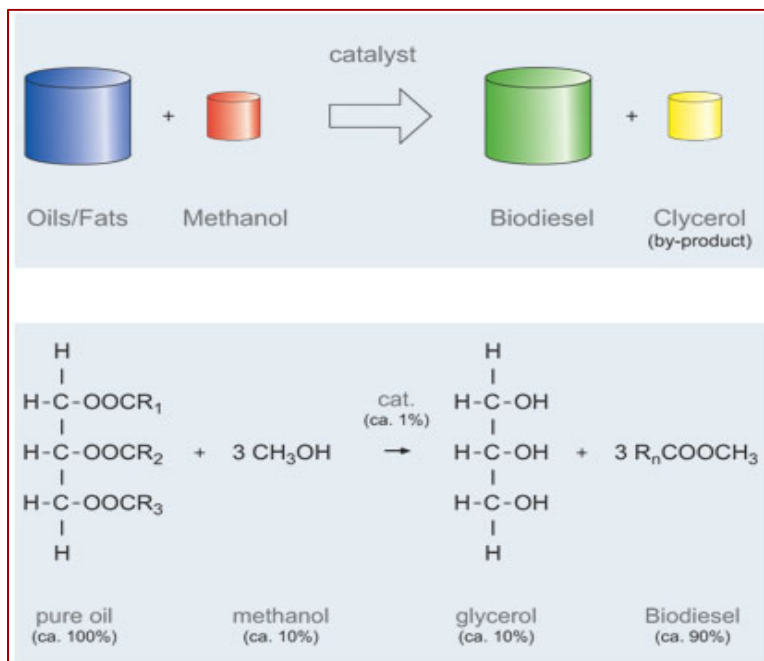


Figure 8: Transesterification process for transforming bio oil into biodiesel (taken from Taiz and Zeiger, 2010).

1.3.2 Future Technologies (AT)

Global research seeks improvements to the biofuel production process in hopes of increasing biofuel production at lower energy inputs. Research has shown promise in using the process known as pyrolysis to produce biofuel from algae. Pyrolysis converts biomass into bio-oil by thermal decomposition of biomass feed in the absence of oxygen using temperatures ranging from 450-500°C (Huang *et al.*, 2009).

Grierson *et al.* (2008) revealed that slow pyrolysis of six different microalgae produced an average of 43% bio-oils by volume for all species studied. Furthermore, the data suggested that the energy required for slow pyrolysis was lower than the energy return of the bio-oil byproducts indicating that slow pyrolysis of microalgae could be a useful renewable energy process.

Liquefaction is also a promising process that has the potential of using less energy than pyrolysis for biofuel production. Since most microalgae contain a high level of moisture when harvesting begins, the microalgae usually need to undergo a drying process before being converted into bio-oil. When moist microalgae are subjected to high temperatures of 300°C, pressures of 10MPa, and catalysts such as NaCO₃ in an aqueous solution, the biomass can be directly converted into biofuel (Huang *et al.*, 2009). Research with *Botryococcus braunii*, a species of green algae, demonstrated that the microalgae liquefaction process produced 57-64% of liquid oils at 300°C, 10MPa with a NaCO₃ catalyst (Huang *et al.*, 2009).

1.3.3 Biofuel Quality (AT)

The biofuels produced by transesterification, pyrolysis, or liquefaction need to be high quality fuels in order to be efficient and economical. If a fuel damages an engine, then it will not survive in the market. Biofuels are graded by six fuel properties: ignition quality, cold- flow properties, heat of combustion, oxidative stability, viscosity, and lubricity (Knothe, 2005).

Knothe (2005) performed extensive research into biofuel quality. The six fuel properties are affected by the structural characteristics of the biofuel's lipid composition. These structural characteristics include chain length, degree of unsaturation, branching of the chains, and configuration of double bonds (Table 4). Knothe (2005) recommends fatty acids with long, saturated, and branched chains such as oleic acid to be used as biofuels due to their positive effects on fuel quality. The ideal algal biofuel should contain or approximate the following fatty acid ratio 5:4:1 of C16:1, C18:1, and C14:0, respectively (Schenk *et al.*, 2008).

Iodine level is an indicator of the unsaturation of a fuel to establish the stability of that fuel. The iodine level of a fuel measures the amount of iodine reacted with 100g of a fuel sample (Schober and Mittelbach, 2007). Iodine reacts with the double bonds of TAGs, so iodine levels above 120 indicate fuels that are susceptible to oxidation.

The energy balance of any fuel is essential to its efficiency, so it is important to find a biofuel source that requires less energy to grow, but produces large quantities of TAGs. It is important to investigate a wide variety of algal sources to find the optimal biofuel feedstock. The quality of the biofuel is also important for success in the energy market. By improving the amount of the best fatty acids for biofuel production in algae, a possible sustainable and economically feasible energy source can be developed.

1.4 An Algal Candidate for Biofuel Production: *Ettlia oleoabundans* (BM)

Oil-producing algal species have gained significant momentum as a potential sustainable source of biofuel. More basic research still needs to be completed on a variety of species in order to begin assessing which species holds the most promise for further

development. *Ettlia oleoabundans* is one such algal species which may prove to be a potential sustainable feedstock for biofuel production.

Table 4: How fuel properties are affected by fatty acid composition in a biofuel (taken from Knothe, 2005).

Fuel Property	Fatty Acid Structural Characteristics	Affects
Ignition Quality (IQ)	chain length; branching	longer chains have higher IQ; branching lowers IQ
Cold-Flow (CF)	chain saturation; branching	higher melting points; crystallize at higher temperatures
Heat of Combustion (HC)	chain length	increases HC
Oxidative Stability (OS)	number and position of double bond	varies the autoxidation
Viscosity (V)	saturation; double bond configuration	increases V; <i>cis</i> double bond increases V
Lubricity (L)	None	fatty acids are good lubricants

1.4.1 *Ettlia oleoabundans* (BM)

Ettlia oleoabundans (UTEX 1185), formerly known as *Neochloris oleoabundans* (Figure 9), is a freshwater unicellular green microalga, which possesses many properties that make it an ideal candidate for alternative energy research. This species was originally isolated from sand dunes in Saudi Arabia (UTEX, 2010) and can produce up to 56% of its dry mass in TAGs (Figure 10) (Gouveia *et al.*, 2009).

E. oleoabundans produces TAGs in its cells. The major fatty acids produced by *E. oleoabundans* are oleic acid (18:1) and linolenic acid (18:3). Only oleic acid is ideal for biodiesel production because it is unsaturated and has a low oxidation rate, resulting in high quality biodiesel. Linolenic acid is not as desirable of a TAG, but it does meet maximum requirements of the European Union Standard for biodiesel by containing only three double bonds in the carbon skeleton. Additionally, the lipids produced by *E. oleoabundans* have an iodine level of 72, indicating that they are relatively stable, thereby further establishing their usefulness as a biofuel source (Gouveia *et al.*, 2009).

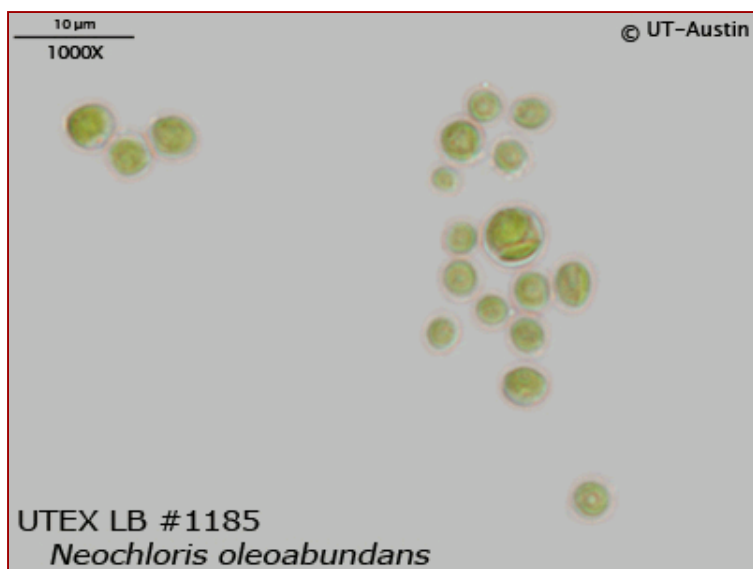


Figure 9: Microalgae *E. oleoabundans* (taken from UTEX, 2010).

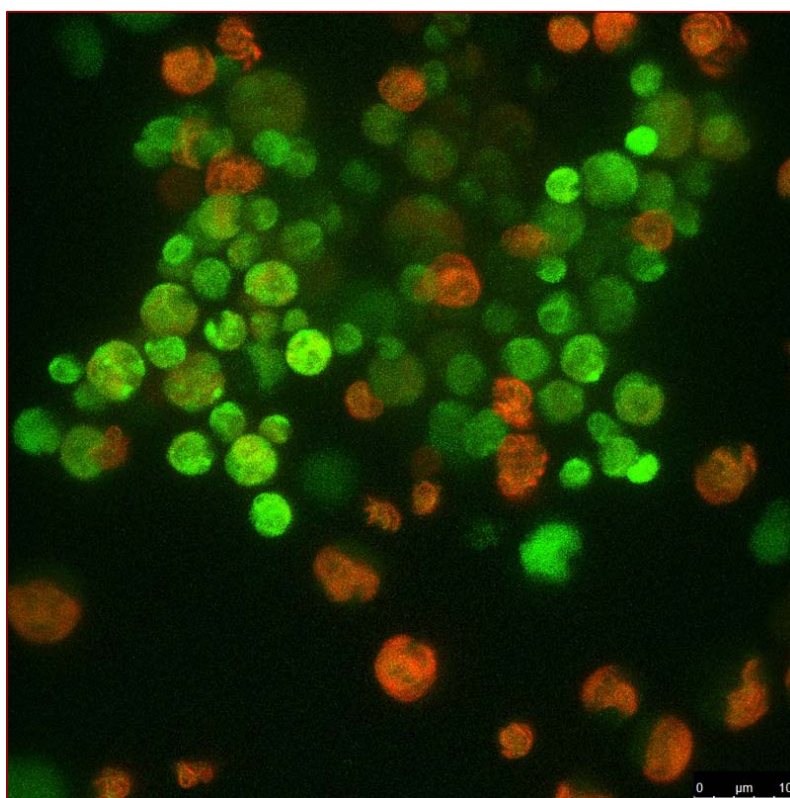


Figure 10: *E. oleoabundans* confocal fluorescence microscope image. Green fluorescence shows chlorophyll, and orange shows oil.

The biomass productivity of *E. oleoabundans* is similar to that of other potential biofuel producing algae. In optimal nitrogen starved conditions, *E. oleoabundans* is capable of very high lipid production when compared to other algal species (Gouveia and Oliveira,

2008). Its growth rate is also high, but not necessarily faster than other algal species. To compare oil-producing microorganism growth rates, *E. oleoabundans* was grown in outdoor ponds in Portugal from May through August and produced 0.09gDW/L/day with a maximum biomass concentration of 2.0gDW/L (Gouveia and Oliveira, 2008). In the same study, the oil-producing filamentous cyanobacteria, *Spirulina maxima*, grew at 0.2gDW/L/day to a maximum concentration of 3.1gDW/L. For comparison the oil producing green algae *Dunaliella tertiolectus* had a growth rate of 0.12gDW/L/day, and a maximum concentration of 3.6gDW/L (Gouveia and Oliveira, 2008). Although the growth rate and biomass yield of *E. oleoabundans* was increased by manipulating culture media, *E. oleoabundans* did not produce as much biomass as either *Spirulina maxima* or *Dunaliella tertiolectus*. *E. oleoabundans* was still concluded to be one of the most promising biofuel-precursor producing organisms studied due to its oil yield and composition (Gouveia and Oliveira, 2008).

Little research has been done on the fundamental biology of *E. oleoabundans* including its lifecycle and ideal growth conditions. When Gouveia *et al.* (2009) studied growth of *E. oleoabundans* in different media compositions and analyzed for nitrate presence, they found the algae produced more oil in lower nitrate concentrations, but algal growth continued past the nitrate drop-off (Table 5). Chlorophyll decreased after nitrate was depleted while the algae were still growing. The samples were grown at $30 \pm 2^\circ\text{C}$ with continuous illumination of $360 \mu\text{mol m}^{-2} \text{s}^{-1}$ (no light model listed) and supplied with a 5% CO_2 enriched air mixture. It was hypothesized that as nitrogen becomes limiting, *E. oleoabundans* begins using their chlorophyll as a nitrogen source to continue molecular development and division (Gouveia *et al.*, 2009). The remaining chlorophyll is then likely converted into the fatty acids and lipids that accumulate in the cell (Li *et al.*, 2008).

Table 5: Summary of cell growth, lipid production, and nitrogen consumption results obtained with media with different sodium nitrate (taken from Gouveia *et al.*, 2009).

Sodium nitrate concentration	3 mM	5 mM	10 mM	15 mM	20 mM
Initial NaNO_3 (mM)	3.23	4.96	10.29	15.58	20.94
Residual aNO_3 (mM)	0	0	0	0.10	4.97
Maximum biomass concentration (g/l)	1.85	2.37	3.15	2.91	2.70
Biomass productivity ($\text{gDW l}^{-1} \cdot \text{day}^{-1}$)	0.31	0.40	0.63	0.58	0.54
Biomass yield (g DCW/g N)	40.91	34.13	21.87	13.43	12.08
Lipid productivity ($\text{gl}^{-1} \cdot \text{day}^{-1}$)	0.125	0.133	0.098	0.044	0.038

1.5 Growth Parameters

As partially illustrated by the above example, many factors affect growth and oil production of algae including inorganic nutrients, CO_2 , temperature, and the amount and

quality of light. This project focuses on two growth parameters, light intensity and temperature, and how they affect the growth and lipid production of *E. oleoabundans*.

1.5.1 Light Intensity (AT)

Light is one of the essential inputs microalgae need to grow and produce bio-oil because it is the driving force for photosynthesis, the process that converts light into chemical energy by fix carbon dioxide into sugars. Understanding this growth parameter is critical to obtaining maximum algal oil production.

1.5.1.1 Algae and the Light Reactions of Photosynthesis

Plants and algae absorb light energy through photopigment complexes known as chlorophylls and carotenoids to power the light reactions of photosynthesis in the cell organelle, the chloroplast. Many different photopigments are found in photosynthetic organisms in order for the organisms to absorb the different wavelengths of light found in sunlight. Chlorophytes (commonly known as green algae) such as *E. oleoabundans* and *B. braunii*, contain both chlorophyll *a* and *b* (Blankenship, 2002). Chlorophyll *a* and *b* act as antennas, gathering light at 430, 680, 453, and 660nm and sending the energy to reaction center complexes embedded in the thylakoid membrane where the light energy powers redox reactions by exciting electrons (Taiz and Zeiger, 2010). These reaction center complexes are called Photosystem I (PSI) and Photosystem II (PSII).

PS I and PS II work in a sequence to shuttle both electrons and protons in and out of a chloroplast's lumen and stroma. PSII absorbs red light (680nm) exciting electrons, which generates energy to oxidize water and producing oxygen. The oxidation of water releases protons, which begins the formation of a proton gradient in the lumen. Electrons also enter a photosystem electron transport chain (ETC) and are carried to PSI. The ETC also generates protons, which increase the electrochemical potential gradient inside the lumen (Taiz and Zeiger, 2010). PSI absorbs far red-light (700nm) to reduce NADP⁺ to NADPH, which is released into the stroma and used in the dark reactions of photosynthesis to fix CO₂, which can ultimately lead to lipid metabolism (Taiz and Zeiger, 2010).

The protons produced during these steps diffuse from the lumen to the stroma through the enzyme, ATP synthase, due to the electrochemical potential gradient produced by the reactions. ATP synthase uses the protons to produce the energy molecule, adenosine triphosphate (ATP), by photophosphorylation. ATP is used by plants and algae to power a variety of metabolic pathways (Taiz and Zeiger, 2010).

1.5.1.2 Algae and the Calvin-Benson Cycle of Photosynthesis

Photosynthetic organisms, including algae, use the energy from the light reactions to power the metabolism of organic compounds during a process called the Calvin-Benson Cycle, the so called dark reactions of photosynthesis. This cycle occurs in three stages in the chloroplasts. Stage 1 called carboxylation, is catalyzed by the enzyme, ribulose-1,5-

bisphosphate carboxylase oxygenase, (Rubisco) and generates a carbon compound named 3-phosphoglycerate from water and CO₂. Next, during the second stage called reduction, 3-phosphoglycerate is phosphorylated by ATP then reduced by NADPH yielding triose phosphates, which can be used to synthesize carbon compounds such as TAGs. The ATP and NADPH used during Stage 2 are synthesized by the light reactions. During the last stage, Rubisco is regenerated in order to keep the Calvin Benson Cycle operating (Taiz and Zeiger, 2010).

1.5.1.3 Regulation of Photosynthesis

Light regulates many enzymes involved in the Calvin Cycle. In their inactive state, several key enzymes needed for the Calvin Cycle contain disulfide bonds. These enzymes can be activated by cleavage of the disulfide bonds by thioredoxin, which can occur when there is a high ratio of reduced thioredoxin to oxidized thioredoxin. This ratio is controlled by the presence of light; the more light available, the higher the ratio of reduced thioredoxin to oxidized thioredoxin. Low levels of light reduce thioredoxin's ability to cleave disulfide bonds in enzymes and increases the formation of inhibitory supramolecular complexes by the enzymes (Figure 11; Taiz and Zeiger, 2010).

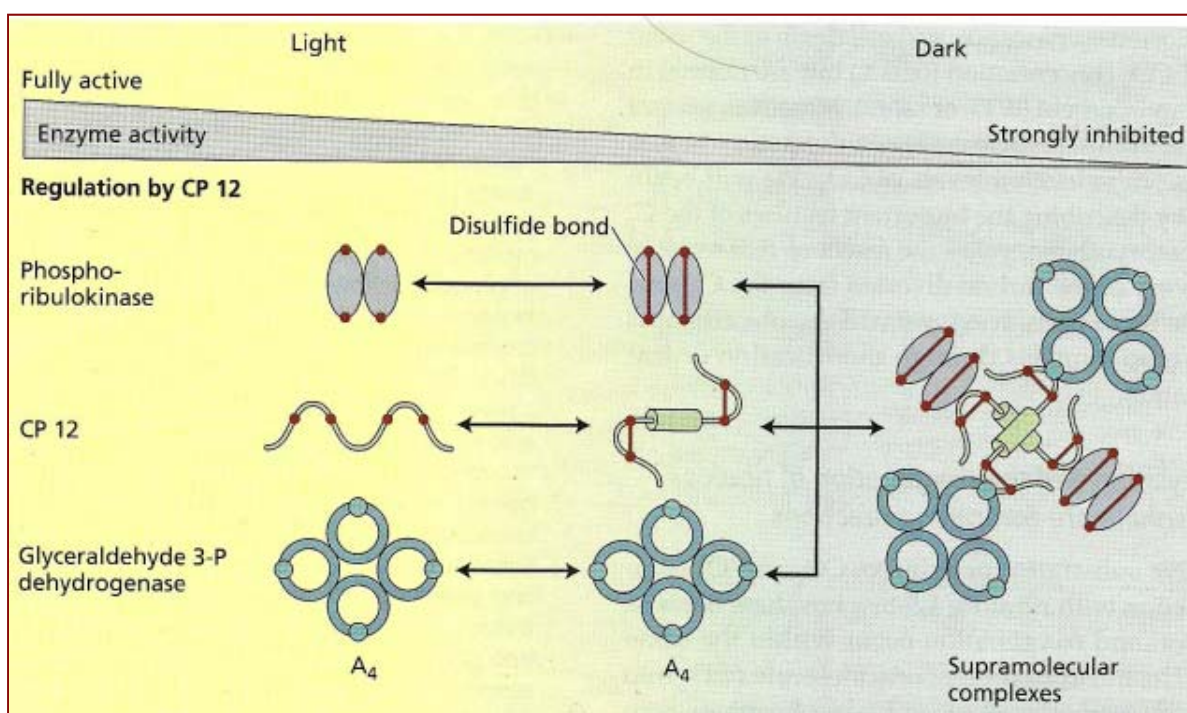


Figure 11: Regulation of the carbon reactions of photosynthesis by light and supramolecular complexes (taken from Taiz and Zeiger, 2010).

The enzyme Rubisco requires ATP to convert the enzyme from its inactive to active form. During this activation process, a carboxyl group is added to a lysine in the L subunit in Rubisco. Rubisco activation requires ATP from the light reactions to lower the ability of

ribulose-1,5-bisphosphate (RuBP) and other inhibitors from binding to inactivate Rubisco, allowing the enzyme to activate (Blankenship, 2002). The more light available, the more active is Rubisco; however, the light saturation point of Rubisco has been reported as $100\mu\text{mol m}^{-2} \text{sec}^{-1}$ (Campbell and Ogren, 1992).

1.5.1.4 Function of Light Intensity

Light intensity is a function of distance from a light source. The further a point is from a light source, the less intense the light is because light is emitted from a source equally in all directions and must spread across more surface area as it travels further away from the source. Distance and light intensity represent an inverse square relationship and is expressed by the following equation (NASA, 2010):

$$I = \frac{L_o}{d^2}, \text{ where } L_o \text{ is the luminosity and } d \text{ is the distance squared}$$

For example, if one moves two feet away from a light source, the light is four times less bright than it was at the original location.

Light intensity can be measured with many different instruments which measure various units of light. Irradiance is the measure of energy that falls at a particular point with units of watts per meter square (Wm^{-2}) (Taiz and Zeiger, 2010). When experimenting with plants, light intensity is usually measured using a light sensor that detects how many photons are emitted from the light source per area. This is called photon irradiance, or photosynthetic photon flux (PPF), which has quantum units of $\mu\text{mol m}^{-2} \text{s}^{-1}$ (Apogee Instruments Inc., 2010).

1.5.1.5 Light Availability

Finding the optimal light intensity for a microalgal species is important because the amount of light directly affects the photosynthesis of microalgae (Wahal and Viamajala, 2010). If microalgae are subjected to an excessive amount of light energy for long periods of time, then PSII can be damaged; this is known as chronic photoinhibition. Chronic photoinhibition can decrease the photosynthetic rates of the organisms by damaging the D Protein of Photosystem II, which causes a malfunction in the electron transport chain of photosynthetic systems (Han *et al.*, 2000). The D1 Protein is part of the photoinhibition repair cycle, but during prolonged exposure to high light intensities, the repair cycle is unable to fix and prevent damage to PSII (Han *et al.*, 2000).

In contrast, if microalgal cultures are not exposed to enough light, then lower rates of photosynthesis can occur (Taiz and Zeiger, 2010). Furthermore, the density of the culture influences the amount of light, which can penetrate the culture; high density cultures shade themselves, so less light enters the center of the culture (Wahal and Viamajala, 2010). This creates uneven measures of PPF in the culture, and in low density

cultures photoinhibition can occur because too much light enters (Wahal and Viamajala, 2010). Indeed, there is an optimum light intensity for optimum growth, but the incident light intensity changes as the culture becomes denser. Thus, control of light intensity can be crucial to survival of microalgae.

Plants growing in different parts of the world are subjected to different amounts of light (Table 6). Furthermore, light intensity outdoors is not constant during every part of the day and year so it cannot be controlled, only anticipated. However, cultures grown within indoor bioreactors can be exposed to a constant and controlled light intensity throughout the day and year. It is important to discover how different light intensities affect algal growth and lipid production to determine which algal species may be successfully grown as a biofuel source in the different parts of the globe. For example, sunlight in the US Northeast differs in the winter and summer; therefore, if an algal species is grown in outdoor bioreactors, it must be able to survive the differences in light to be a successful fuel source.

Table 6: Average photosynthetic photon flux (PPF) for healthy plant growth (taken from Apogee Instruments Inc., 2010).

Type of Plant/ Condition	Approximate PPF For Good Growth ($\mu\text{mol m}^{-2} \text{s}^{-1}$)	Daily PPF ($\text{mol m}^{-2} \text{d}^{-1}$)
House plants	30 to 200	3 to 20
Leafy crop plants (lettuce and basil)	200 to 600	10 to 30
Tomatoes and other fruit crops	400 to 1000	20 to 50
Full sunlight at noon in the summer	2000	50 in midsummer; 25 inside a good glass greenhouse
Full sunlight at noon in the winter	~1200	10 in midwinter; 5 inside a good glass greenhouse

Further complicating the light intensity aspect of growing algae is CO_2 concentration. Each plant species has what is termed a CO_2 compensation point, the balance between photosynthesis and respiration where the partial pressure of CO_2 in the cell determines if the cell can grow. Below the compensation point the cells die, above it cells will grow and add biomass. As light intensity increases, the CO_2 level must also

increase in order to increase biomass until the upper limits of the system are reached. Once the upper limit of the system is reached, the plant is saturated with CO₂ and photosynthesis can no longer increase (Taiz and Zeiger, 2010).

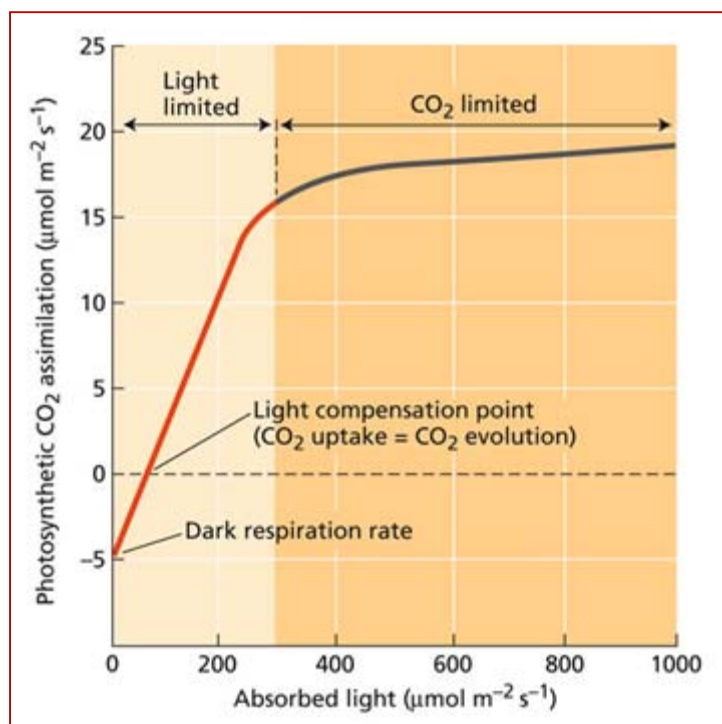


Figure 12: The Effects of CO₂ on photosynthesis (taken from Taiz and Zeiger, 2010).

1.5.1.6 Past Studies

A number of studies have shown the different effects light intensity has on microalgae species ranging from growth rates to total fatty acid content. For example, Sorokin and Krauss (1957) compared the effects of a wide range of light intensities on six species of green algae: *Chlorella pyrenoidosa*, *Chorella vulgaris*, *Scenedesmus obliquus*, *Chlamydomonas reinhardtii*, and *Chlorella pyrenoidosa*. Each species was grown under light intensities ranging from 0-21523 $\mu\text{mol m}^{-2} \text{sec}^{-1}$ and supplied with 4% CO₂ in air mixture. Fluorescent bulbs provided the light for 0-258 $\mu\text{mol m}^{-2} \text{sec}^{-1}$ experiments and incandescent for the 258-21523 $\mu\text{mol m}^{-2} \text{sec}^{-1}$ experiments. Temperature was controlled by placing the test tubes in water baths. All experimental strains except for *C. pyrenoidosa* were only grown at 25°C; however, *C. pyrenoidosa* was grown at 25 and 39°C. Optical density readings at 600nm were taken and converted into growth rates, which were compared and varied greatly between the algal species. According to the results found in Sorokin and Krauss (1957), the six algal species under experimentation obtain maximum growth at the lower light intensities which indicates that these algal species can survive in shaded, low light areas and can potentially be grown in mass cultures without suffering penalties from high culture densities. Furthermore, the results showed for the same

species, such as *C. vulgaris*, that increasing the light intensity did not increase the growth rate.

Van Baalen *et al.* (1970) analyzed heterotrophic growth of two cyanobacteria, *Agmenellum quadruplicatum* and *Lyngbya lagerheimii* under dim and high light conditions. Cultures of *A. quadruplicatum* and *L. lagerheimii* were grown in test tubes supplied with 1% CO₂ in air under 450 $\mu\text{mol m}^{-2} \text{sec}^{-1}$ to simulate high light conditions then at 12.9 $\mu\text{mol m}^{-2} \text{sec}^{-1}$ to simulate dim light conditions. For each light condition, the algae cultures were grown both with and without glucose. The dry weights of the cultures were determined and the cultures grown in the low light conditions exhibited no autotrophic growth, but when supplied with glucose, *L. lagerheimii* cultures had a longer generation time of 60 hours, double the amount of time the high light cultures took, which was 30 hours. Cultures grew heterotrophically. When another species, *A. quadruplicatum*, was grown in dim light with glucose, the generation time was 55 hours. High light intensity, however, yielded a generation time of 2.9 hours \pm glucose. These results indicated that the growth of *A. quadruplicatum* and *L. lagerheimii* was inhibited at low light intensities, 12.9 $\mu\text{mol m}^{-2} \text{sec}^{-1}$.

Solovchenko *et al.* (2007) grew cultures of the fresh water algae, *Parietochloris incise*, at three different light intensities, 35, 200, and 400 $\mu\text{mol m}^{-2} \text{s}^{-1}$ in both nitrogen-containing and nitrogen-deficient media. The cultures were grown at 25°C and supplied with 1% CO₂. Differences in growth and total fatty acids in the cultures were measured. Their data revealed that in nitrogen containing medium, cultures of *P. incise* grown at a high light intensity of 400 $\mu\text{mol m}^{-2} \text{s}^{-1}$ for 14 days produced 50-200% more fatty acids than cultures grown at 35 and 200 $\mu\text{mol m}^{-2} \text{s}^{-1}$, respectively. At the 400 $\mu\text{mol m}^{-2} \text{s}^{-1}$ light intensity, lack of nitrogen inhibited fatty acid production. Solovchenko *et al.* (2007) suggested that the cultures grown under 400 $\mu\text{mol m}^{-2} \text{s}^{-1}$ and supplemented with nitrogen are more productive and efficient than the other cultures because they convert the excess light energy into TAGs, possibly to prevent photo-oxidative damage.

In another example, Qin (2005) grew *B. braunii* at nine different light intensities and measured the generation time and relative total lipid content (rTLC) of each culture. The cultures were grown at 23°C with 12 hours of light and 12 hours of dark. The algal cultures reached their optimum growth rate and relative total long chain hydrocarbon content at 175 $\mu\text{mol m}^{-2} \text{s}^{-1}$. At 175 $\mu\text{mol m}^{-2} \text{s}^{-1}$, the cultures had the lowest generation time of 2.5 days while cultures greater of less than 175 $\mu\text{mol m}^{-2} \text{s}^{-1}$ increased in generation time. Furthermore, at 176 $\mu\text{mol m}^{-2} \text{s}^{-1}$, the rTLC was approximately 0.8, and as the light intensity increased above 175 $\mu\text{mol m}^{-2} \text{s}^{-1}$, the rTLC declined. Their study suggested that cultures growing in low light (< 175 $\mu\text{mol m}^{-2} \text{s}^{-1}$) were growth inhibited while the cultures growing at high light (> 175 $\mu\text{mol m}^{-2} \text{s}^{-1}$) experienced photoinhibition (Qin, 2005).

1.5.2 Temperature (BM)

Although the effect of temperature on algal growth is not, to our knowledge, a well-studied area, several studies have provided some insights. For example, Bosma *et al.*, (2007) studied the effects of light on algal growth while also recording temperature readings. Their results showed that when the temperature in a bioreactor growing *Monodus subterraneus* fluctuated, changes in growth rate and photosynthetic yield were also observed. The data suggested there was an ideal temperature for peak growth. Similarly, when *B. braunii* was grown at different temperatures, both growth and lipid production were affected. The most rapid growth rate and highest lipid production were both achieved at 23°C (Qin, 2005).

Goldman and Carpenter, (1974) provided an early attempt to develop a mathematical model for the relationship between temperature and growth. Their analysis used data from published studies and indicated the relationship is unique for each species. Therefore the effects of temperature on potential algal biofuel candidates must be gathered for each species in order to optimize growth.

Eppley (1972) performed a similar study on saltwater phytoplankton. His results showed that there is an upper limit on temperature for algal growth. Like Goldman and Carpenter, Eppley pooled results from a number of sources, and observed a similar trend in algal growth and temperature, the growth rate usually increases as temperature increases. Above 40°C, Eppley discovered that phytoplankton growth among a number of species plummets, and some decline closer to 35°C. These results suggest that temperature is indeed an important factor in algal growth, and that the exact relationship can vary greatly from species to species with regards to the trend and limits.

Bosma *et al.*, (2007) hypothesized that the effects of temperature on algal growth were a result of an impact on photosynthetic rates within the algae. Their hypothesis focused on the rate of enzymatic reactions affected by temperature, so that “At sub-optimal temperatures, light was absorbed by photosystems, but could not be converted to carbohydrates by enzymes due to lower enzyme activities.” (Bosma *et al.*, 2007). Rubisco is a slower functioning enzyme in the Calvin Cycle, and thus acts as one of the major rate-limiting steps in photosynthesis. Temperature is known to affect enzymatic activity at both extremes. At very low temperatures, enzyme activity can be slowed due to slower movements of molecules in the system. Since enzymes are proteins, high temperatures may denature the enzyme, resulting in functional failure. Bernacchi, *et al.*, (2001) demonstrated that Rubisco activity in leaf tissue is actually quite sensitive to high temperatures and in *Nicotiana tabacum* is inhibited at 35°C. Thus, finding an ideal temperature for growing algae may be identification of the temperature for optimum Rubisco activity.

Chapter 2: Hypotheses and Objectives (AT, BM)

The goal this project was to determine the light intensity and temperature conditions at which to grow an oil producing species of algae for high productivity of biomass and oil yield and composition. The following hypothesis will be tested during this project:

1. If there is an optimal temperature and light intensity for *E. oleoabundans* growth and lipid production then this species can likely be optimized for biofuel production.

From this hypothesis, the following objectives were formed:

1. Determine the temperature that yields optimal growth and fatty acid composition, and lipid concentration for *E. oleoabundans* between 5, 15, 25, and 35°C.
2. Determine the light intensity that yields optimal growth and fatty acid composition, and lipid concentration for *E. oleoabundans* between 70, 130, and 200 $\mu\text{mol m}^{-2}\text{sec}^{-1}$.

Chapter 3: Methods

3.1 Maintenance of Stock Cultures (AT, BM)

Stock cultures of 30ml of *E. oleoabundans* (UTEX 1185) were maintained in 125mL Erlenmeyer flasks with Bold's Basal Media (BBM) (Appendix A) on a rotary shaker at 25°C at 100rpm to allow for proper aeration and to prevent settling of the algae. BBM was selected as growth media because it was shown in other work done in the lab to promote reasonable growth of this species (Yang et al., 2011).

Every two weeks, 5mL of the algal stock culture was subcultured and inoculated into 25mL of BBM. During every other round of subculturing, a contamination check was made by streaking samples of culture onto Petri dishes of BBM containing 20g/l plant tissue culture agar (Carolina, product number 198206) and placed under a cool white fluorescent light (Phillips 51518) at 25°C. Every 4 weeks cultures samples were also streaked on LB media containing 15g/l plant tissue culture agar in order to stimulate the growth of any contaminating bacteria.

3.2 Light Intensity and Temperature (AT, BM)

To investigate the optimal light intensity and temperature for *E. oleoabundans* that would result in the highest productivity, yield, and lipid production, the following experiments were designed. Week old cultures for both species were diluted to OD of 0.1 and aliquoted into 12 125mL Erlenmeyer flasks as the experimental inoculants. The experimental flasks were grown in a Percival Scientific Incubator (model number AR-60L)

on a rotary shaker bed at 100rpm until they reached stationary growth phase and produced lipids. The temperatures tested were 5, 15, 25, and 35°C. At each temperature, the light intensities investigated were 70, 130, and 200 $\mu\text{mol}/\text{m}^2\text{sec}^{-1}$. Four flasks were individually measured and then placed at each light intensity tested (Figure 13) Preliminary data (unpublished) showed that *E. oleoabundans* grew faster when there was more red light emitted from the source, so the light was continuously provided by a 15 Watt GE Kitchen & Bath Starcoat® T8 (Appendix B).

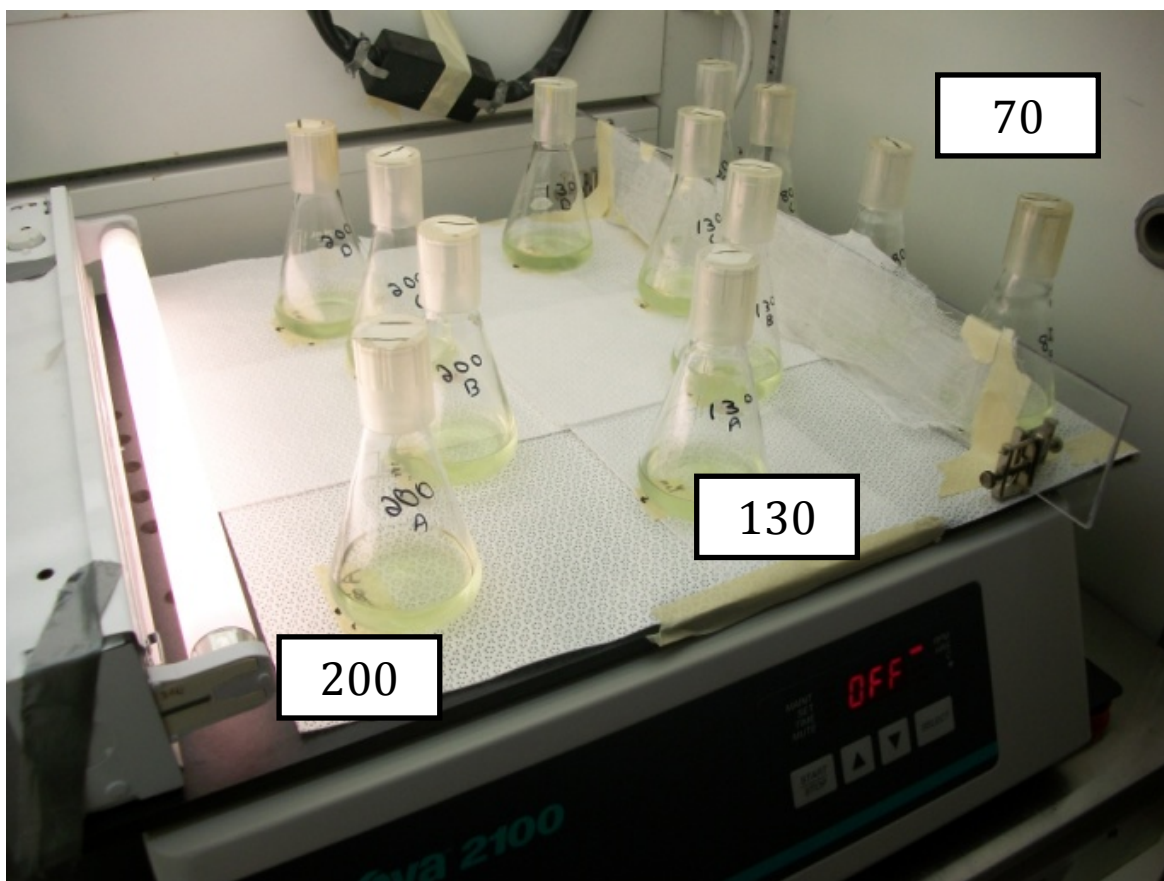


Figure 13: Experimental setup. Light intensities are measured in $\mu\text{molm}^{-2}\text{sec}^{-1}$.

3.3. Growth Analysis (AT, BM)

Algal growth of each culture was determined by OD_{540} readings. Samples of 1mL were sterilely collected from each flask and the optical density measured using an Hitachi U-2800 Double Beam Spectrophotometer (model number 122-002). The OD_{540} readings for each temperature run were converted into Cell Dry Weight by using the formula as described by Yang *et al.* (2011) where,

$$\text{OD}_{540} = 1.3071 \text{ gDWL}^{-1}.$$

Primary productivity is the generation of organic matter from inorganic nutrients such as CO₂, nitrate and phosphate by plants and algae. For *E. oleoabundans* to be a feasible candidate for biofuel, the algae need to have high productivity. The primary productivity of the algae cultures in the temperature runs was determined for each light intensity using the cell dry weight data using the following formula:

$$\frac{\text{Initial DW} - \text{Highest DW}}{\text{Duration}} = \text{Productivity (DWL}^{-1}\text{Day}^{-1}\text{)}$$

The biomass yield of a biofuel candidate is also a key to feasibility. Biomass yield is a ratio between the biomass produced (productivity) and substrate (nutrients in the BBM) consumed by the algae during the runs. After the productivity was calculated, the biomass yield was determined:

$$\text{Productivity} \times \text{Starting Volume in Flask} = \text{Biomass Yield (DWDay}^{-1}\text{)}$$

3.4 Oil Concentration (AT, BM)

Lipid concentrations were approximated using the Nile Red Fluorescence Assay Protocol (Appendix C). Nile red fluorescence allows for comparison of lipid levels between samples, but does not yield a qualitative result. Fluorescence was measured by a Perkin Elmer Wallac 1420 Multilabel Counter Fluorometer (model number 1420-050). Oleic Acid Equivalents (OAE) are a unit developed by Yang et al. (2011) to describe oil presence in an algal culture using Nile red fluorescence readings. The equation for OAE follows:

$$\text{OAE (mg/L)} = \frac{\text{Nile red Reading} + 6655}{209.43}$$

Dry weight is calculated from the algal growth tables where OD is correlated to dry mass, and %oil/algae is calculated by dividing the OAE by the DW and multiplying by 1000.

3.5 Gravimetric Analysis (AT, BM)

After reaching stationary phase, lipids were extracted using the Lipid Gravimetric Determination Protocol (Appendix D). This process measured lipid dry weight per dry weight of algae. These lipid dry weights were normalized by the volume of harvested culture and are presented here in terms of lipid concentration (mg/L).

3.6 End Media Analysis (AT, BM)

Nitrate and phosphate levels in the end media were measured after Gravimetric analysis following Nitrate Analysis (Appendix E) and Phosphate Analysis Protocols (Appendix F). End media pH was measured using an Accumet pH meter (model 1S).

3.7 Gas Chromatography-Mass Spectrometry (AT, BM)

The extracted lipids were then analyzed to determine amount and type of fatty acids following the method of Yang et al. (2011) using Gas Chromatography-Mass Spectrometry

(GC-MS), (GC: Agilent Technologies 7890A GC System, MS: Agilent Technologies 5975CVLMSBWL). The dry extractives were methylated. The column used was a Stabilwax Cat#10623 (30 m x 0.25 mm x 0.25 lm) with polyethylene glycol as the stationary phase.

GC-MS results were used to calculate total and specific fatty acids per extractive (w/w) using the following formula:

$$\frac{\text{Weight Fatty Acid}}{\text{Weight extractives}} \times 100\% = \%FA \text{ per extractives}$$

Results were also calculated for percent fatty acid per lipids harvested from the extraction.

$$\frac{\text{Weight Fatty Acid}}{\text{Weight lipids extracted}} \times 100\% = \%FA \text{ per lipids}$$

3.8 Statistical Analysis (AT, BM)

All experiments were run at least in triplicate. Results were analyzed using the ANOVA test, performed using IBM's SPSS 17 Statistics software.

Chapter 4: Results (AT, BM)

4.1 Growth of *Ettlia* at 4 temperatures and 3 light intensities.

To measure the growth of the algal cultures, first the average OD₅₄₀ readings were converted into cell dry weight measurements (g/L). At the three highest temperatures (15, 25, and 35°C), and light intensities (70, 130, and 200 μmol/m² sec⁻¹), *E. oleoabundans* exhibited growth (Figure 14). No growth was observed at 5 °C at any light intensity. Indeed cultures rapidly bleached within about 3-5 days, with the fastest rate of bleaching at the highest light intensity (data not shown). Interestingly when the 5 °C cultures were subsequently transferred to a shaker at 25 °C, they all recovered and began to grow again after about a week at the higher temperature (data not shown). As shown in Figure 14, there was substantial algal growth at 15°C and 25°C, but not at 35°C. The growth results for 25°C in particular showed fluctuating growth curves; this was in contrast to what was expected to be a smooth growth curve.

The peak average cell dry weights for each sample are presented in Table 7. These dry weights demonstrated the maximum algal biomass harvested from each sample at different times under these culture conditions. Statistical analysis did not show any significant difference between growth at the different light intensities for any specific temperature; however, there is a significant difference in growth at different temperatures.

For example, at the same light intensity, the 35°C peaks are significantly lower than the 15°C and 25°C peaks, but 15°C and 25°C are not significantly different from each other.

Biomass productivity and yield were calculated from the peak dry weights for each culture condition and are presented in Table 8. Again, statistical analysis did not show any significant difference between the light intensities for each temperature; however, there is again a significance difference between the temperatures. For both productivity and yield, the 35°C results are significantly lower than the 15°C and 25°C peaks, but 15°C and 25°C are not significantly different from each other.

The data indicated that 35°C is detrimental to *E. oleoabundans* growth. After three days of growth, the flasks in light intensities 200 and 130 $\mu\text{mol m}^{-2} \text{sec}^{-1}$ in 35°C began bleaching while the flasks at 70 $\mu\text{mol m}^{-2} \text{sec}^{-1}$ were still a healthy green. The bleaching of the 200 $\mu\text{mol m}^{-2} \text{sec}^{-1}$ and 130 $\mu\text{mol m}^{-2} \text{sec}^{-1}$ groups continued through the rest of the experiment. At seven days, the cultures at 200 $\mu\text{mol m}^{-2} \text{sec}^{-1}$ were completely bleached and cultures at 130 $\mu\text{mol m}^{-2} \text{sec}^{-1}$ still retained a slight yellow hue. At 70 $\mu\text{mol m}^{-2} \text{sec}^{-1}$ cultures were only slightly bleached (Figure 15). Overall, the maximum biomass yield, productivity and growth rate were all at 15 °C and 130 $\mu\text{mol m}^{-2} \text{sec}^{-1}$.

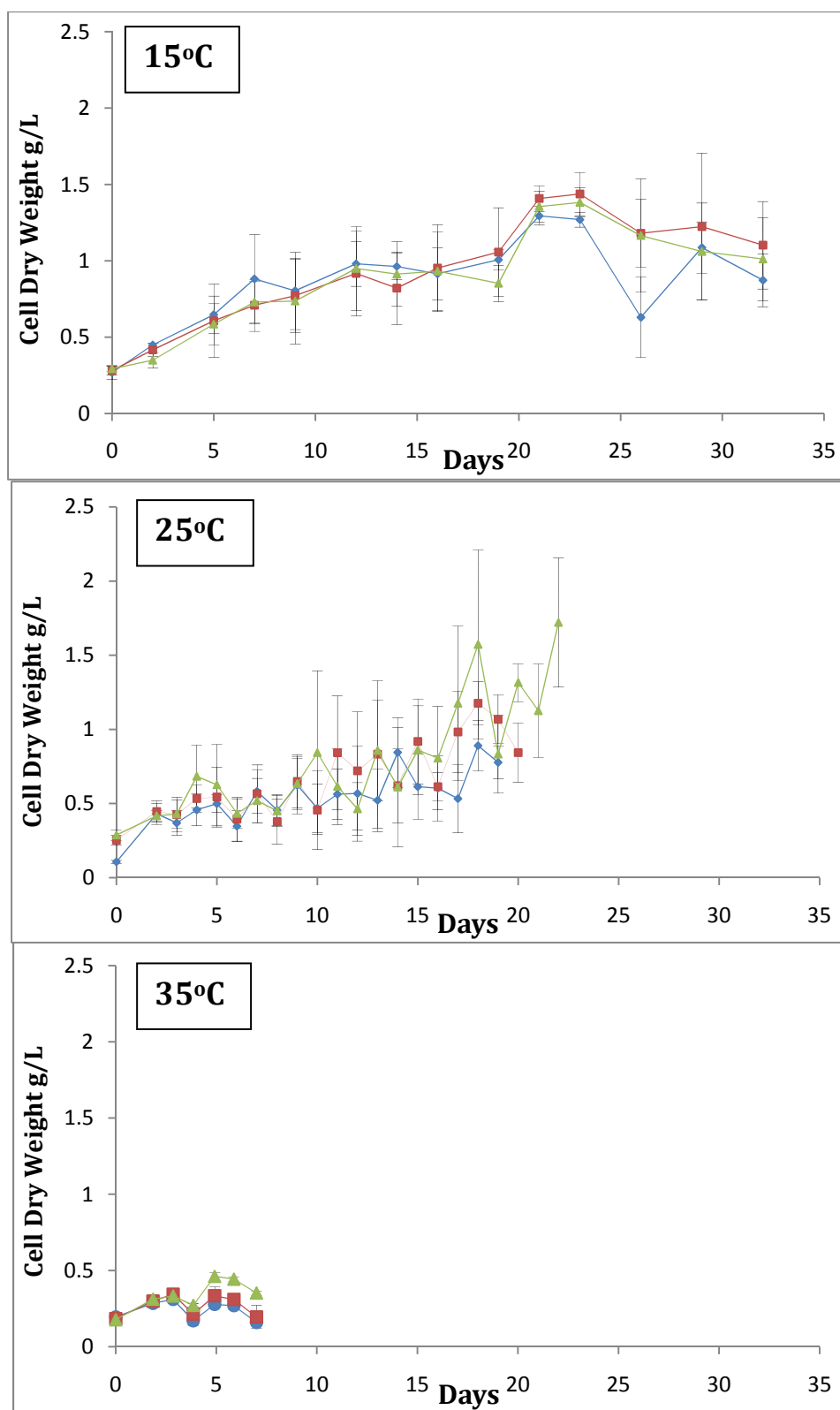


Figure 14: Average cell dry weights (g/L) of *E. oleoabundans* grown at 15°C, 25°C; and 35°C for 70 (triangles), 130 (squares), and 200 (circles) $\mu\text{mol/ m}^2 \text{sec}^{-1}$.

Table 7: Peak Average Dry Weights. Asterisk (*) indicates that the 35°C values were significantly lower than for 15°C and 25°C ($p \leq 0.05$).

Temperature (°C)	15			25			35 *		
Light Intensity ($\mu\text{mol}/\text{m}^2 \text{sec}^{-1}$)	70	130	200	70	130	200	70	130	200
DW (g/L) Peak	1.38	1.44	1.29	1.72	1.18	1.57	0.46	0.34	0.31
Day	23	23	21	22	18	18	5	3	3

Table 8: Biomass productivity and yield for each experimental run. Asterisk (*) indicates that the 35°C values were significantly lower than for 15°C and 25°C ($p \leq 0.05$).

Temperature (°C)	15			25			35 *		
Light Intensity ($\mu\text{mol}/\text{m}^2 \text{sec}^{-1}$)	70	130	200	70	130	200	70	130	200
Productivity (DW*L ⁻¹ *Day ⁻¹)	1.37	1.43	1.28	1.71	1.16	0.88	0.06	0.05	0.02
Yield (DW*Day ⁻¹)	54.76	57.01	51.27	51.25	34.91	26.54	1.71	1.60	0.49

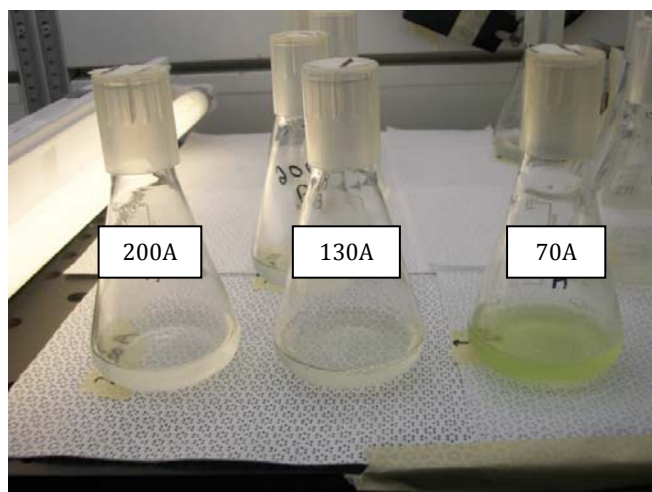


Figure 15: Flask A from each light intensity at 35°C at day seven, demonstrating changes in culture color.

4.2 Oil Detection and Analysis

Nile red fluorescence was used to measure relative oil presence within the cultures. The plots for oil presence are presented in Figure 16. A Nile red reading below 30,000 is outside of the baseline range of the machine for this test with *E. oleoabundans* (Yang et al., 2011), indicating a low but not accurately determinable oil level. Cultures grown at 35°C

only just reached 30,000 at the $200 \mu\text{mol m}^{-2} \text{sec}^{-1}$ peak, which was not considered valid. For the 15°C the oil levels were detectable after 20 days, and for 25°C they were detectable after 12 days.

The peak Nile red results indicated the highest level of oil recorded in the culture. Statistical analysis did not show any significant difference between the light intensities for each temperature; however, there is a significant difference for these results between temperatures. Oil yields are significantly lower for the 35°C cultures vs. the 15°C and 25°C cultures. This was expected since the Nile red readings for the 35°C cultures did not extend beyond baseline. The 15°C and 25°C cultures were not significantly different from each other. Maximum oil production was in cultures grown at 25°C and $70 \mu\text{mol m}^{-2} \text{sec}^{-1}$, rather low temperature and light levels.

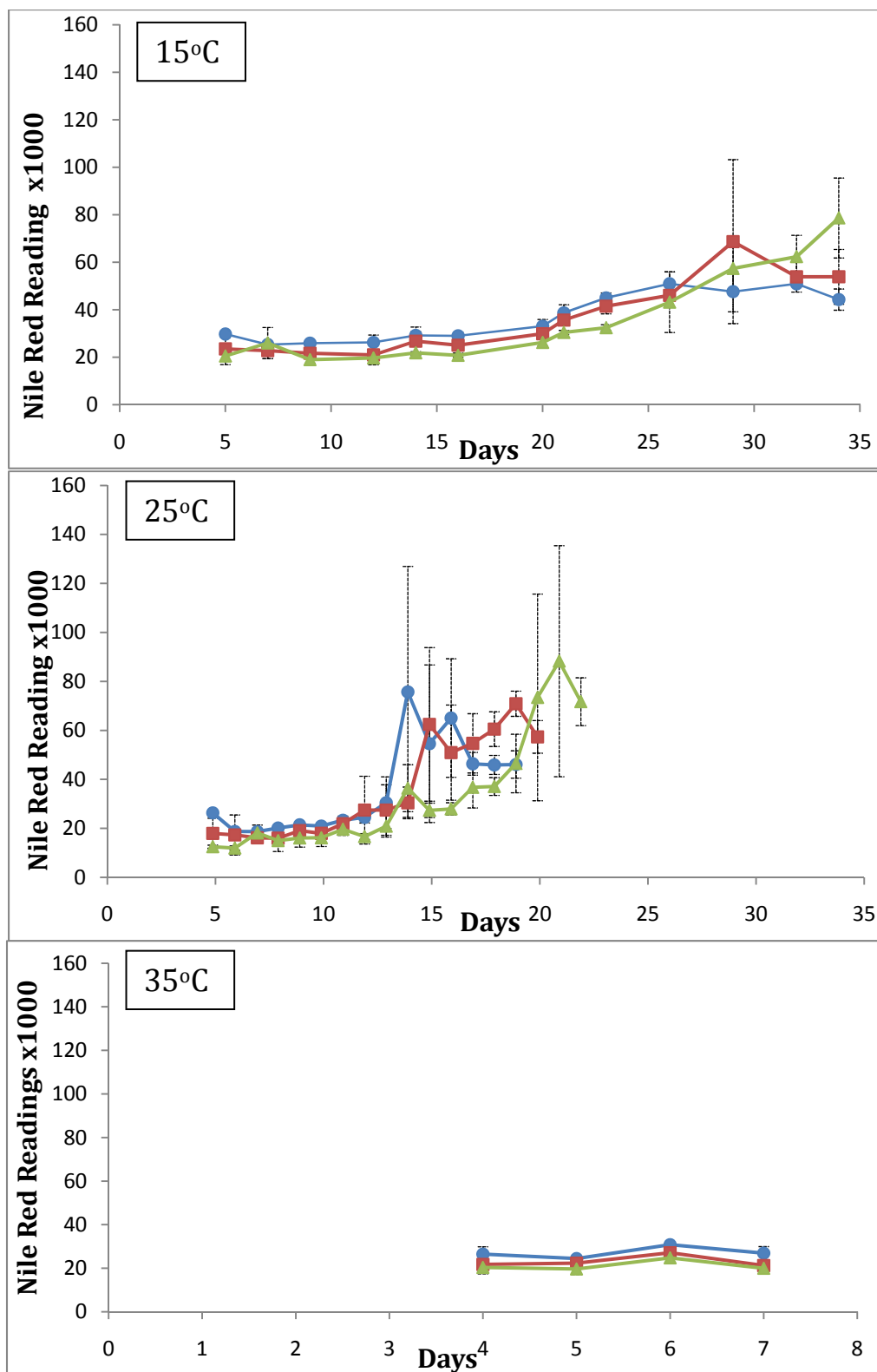


Figure 16: Average Nile red fluorescence readings of *E. oleoabundans* grown under 15°C, 25°C, and 35°C for 70 (triangles), 130 (squares), and 200 (circles) $\mu\text{mol}/\text{m}^2\text{sec}^{-1}$. Readings below 30,000 are not considered valid because they are below the threshold range for this assay.

Table 9: Nile red peak readings. Asterisk (*) indicates that the 35°C values were significantly lower than for 15°C and 25°C (p≤0.05).

Temperature	15°C			25°C			35°C *		
Light Intensity (μmol/m ² sec ⁻¹)	70	130	200	70	130	200	70	130	200
Nile red (fluorescent units)	78653	68682	50938	88262	62448	75710	24768	26075	30811
Time (days)	34	29	26	21	15	14	6	6	6

The changes in the relative percentages of fatty acids in the extracted oil per algal dry mass and the extractives per algae are shown in Table 10. Percent oil per algal dry mass was calculated for the peak average Nile red result from each condition. It indicates the most oil that was present in the sample per algal biomass. Extractives per algal dry mass were calculated from the lipid dry weights recorded after gravimetric analysis. Statistical analysis could not be performed on the extractives per algae results because the gravimetric analysis was performed on pooled samples for each condition; n=1. The extractives per algae results for cultures grown at 35°C at 130 and 200 μmol m⁻² sec⁻¹ were not valid and indicate some error in the extraction process. The weight of the extracted material was greater than the calculated weight of algal cells at the end time point. The likely cause for this error is some contamination or incomplete separation during extraction. Consequently the oil composition data are also presented as % of total FAMES. Besides exhibiting poor growth, the 35°C cultures also failed to produce a measurable amount of oil.

Table 10: Comparison in peak % oil and extractives per algae. ND indicates no data because the Nile red readings did not rise above 30000. The Nile red % was calculated using the OAE formula.

Temperature	15°C			25°C			35°C		
Light Intensity (μmol m ⁻² sec ⁻¹)	70	130	200	70	130	200	70	130	200
Peak %oil/g algae from Nile red	52.63	55.93	50.77	40.26	44.78	56.72	nd	nd	nd
Extractives per algae (%w/w) from extraction	20.94	5.99	21.31	5.15	7.59	11.37	17.52	nd	nd

4.3 Oil Composition

To determine the fatty acids present in the extracted oils, the extract is methylated to yield fatty acid methyl esters (FAMES) prior to separation, identification, and quantification using GC-MS. The GC-MS results for 15 and 25°C are presented in Table 11, showing the percent of each specific fatty acid per total lipids from each extraction. Each

extracted sample contained C18:1, oleic acid, which shows that the best precursor to biodiesel was produced in every condition. At 25°C the 70 $\mu\text{mol m}^{-2} \text{sec}^{-1}$ light intensity was the only condition that yielded C14:0, C16:1, and C18:1, the three fatty acids most desirable for biofuel production. The ideal ratio of these fatty acids for fuel production is 5:4:1 for C16:1, C18:1, and C14:1, respectively (Schenk *et al.*, 2008). The results of this study show a ratio of 0.08: 1.16: 0.05.

The 35°C extraction results have some error from the gravimetric analysis, as mentioned in Section 4.2. Percent lipids per extractives could not be calculated because the extractive weights came out to be more than the final cell dry weight for two of the three conditions, leading us to discount the 17.52% value at 70 $\mu\text{mol m}^{-2} \text{s}^{-1}$ as well. GC-MS analysis still indicated that there were lipids present, so those results are presented in terms of percent specific lipids per total lipids detected, ignoring the relationship between lipids and extractives. The dry extractives contained more than just lipids because the extraction purification process also yields other fats such as chlorophyll (Yang, 2011). Furthermore, there is often contamination from cell wall debris.

Oil composition data were also expressed as percent specific fatty acid per lipid extracted (Table 12). This allowed a comparison between the different conditions to highlight any shifts in the type of oil produced. The data from the 35°C cultures further confirm that the algae were negatively affected by the high temperature, and that the 70 $\mu\text{mol m}^{-2} \text{sec}^{-1}$ was less affected than the two higher light intensities. Of particular interest is the apparent increasing shift to mainly C16:0 and C18:0 at the 130 and 200 $\mu\text{mol m}^{-2} \text{sec}^{-1}$ light intensities at 35°C.

Table 11: GC-MS results for 15°C and 25°C presented as percent specific FAME per extractive. C18:1 is highlighted because it is the most important fatty acid for biofuel production. Orange indicates the condition that yielded all three desired fatty acids for biodiesel.

°C	Light Intensity μmol m ⁻² sec ⁻¹	C14:0	C15:0	C16:0	C16:1	C16:2	C16:3	C17:0	C18:0	C18:1 ω 9	C18:2 ω 6	C18:3 ω 3	Lipids/ Extractive (%w/w)	Extractives/ Algae (%w/w)
		FAMES as % of total extractives												
15	70	0.00	0.00	0.82	0.06	0.03	0.05	0.12	0.14	1.05	0.36	0.11	2.73	20.94
	130	0.00	0.00	2.24	0.15	0.06	0.20	0.35	2.17	2.05	0.95	0.53	8.71	5.99
	200	0.00	0.00	0.53	0.04	0.02	0.06	0.09	0.07	0.45	0.23	0.16	1.65	21.31
25	70	0.05	0.00	1.60	0.08	0.00	0.00	0.12	0.35	1.16	0.42	0.07	3.85	5.15
	130	0.00	0.00	3.39	0.00	0.00	0.00	0.36	0.56	2.00	0.49	0.00	6.79	7.59
	200	0.00	0.00	1.51	0.10	0.10	0.06	0.18	0.27	2.59	1.08	0.25	6.13	11.37

Table 12: GC-MS results for 15, 25, and 25°C presented as percent specific FAME per lipids. C18:1 is highlighted because it is the most important fatty acid for biofuel production.

°C	Light Intensity μmol m ⁻² sec ⁻¹	C14:0	C15:0	C16:0	C16:1	C16:2	C16:3	C17:0	C18:0	C18:1 ω 9	C18:2 ω6	C18:3 ω3	
		FAMES as % of total lipids											
15	70	0.00	0.00	29.87	2.30	0.93	1.78	4.28	5.08	38.63	13.10	4.03	100
	130	0.00	0.00	25.72	1.75	0.70	2.35	4.03	24.96	23.54	10.87	6.08	100
	200	0.00	0.00	32.08	2.43	0.93	3.44	5.63	4.40	27.53	13.94	9.62	100
25	70	1.35	0.00	41.48	2.19	0.00	0.00	3.08	9.02	30.22	10.95	1.72	100
	130	0.00	0.00	49.94	0.00	0.00	0.00	5.32	8.17	29.38	7.19	0.00	100
	200	0.00	0.00	24.54	1.67	1.65	1.00	2.93	4.35	42.16	17.65	4.05	100
35	70	2.72	1.24	28.71	1.57	0.00	3.35	1.73	9.16	12.09	29.49	9.92	100
	130	0.00	0.00	52.23	0.00	0.00	0.00	0.00	12.38	35.40	0.00	0.00	100
	200	0.00	0.00	60.09	0.00	0.00	0.00	0.00	39.91	0.00	0.00	0.00	100

Chapter 5: Discussion (AT, BM)

The results from this study agreed with others performed on oil producing algae; however, since experimental designs differ, such as CO₂ supplementation, not all data from our experiment are directly comparable to past studies. As previously described, Gouveia and Oliveira (2008) compared *E. oleoabundans* growth to other algal species growing in outdoor ponds. They calculated productivity and peak biomass for each species. Their productivity and peak biomass are compared to this project's results in Table 13. Gouveia and Oliveira (2008) measured a productivity that was substantially lower than our results at 15°C and 25°C. Our highest productivity occurred in cultures growing in 25°C under 70 $\mu\text{mol m}^{-2} \text{sec}^{-1}$ light, 1.71 gDW L⁻¹ day⁻¹, which is almost twenty times higher than their peak of 0.09 gDW L⁻¹ day⁻¹. However, Gouveia and Oliveira (2008) obtained a higher peak biomass of 2.00 gDW L⁻¹ compared to our highest which was 1.71 gDW L⁻¹ growing in 25°C under 200 $\mu\text{mol m}^{-2} \text{sec}^{-1}$. The differences in productivity and peak biomass may be attributed to the growing conditions of the cultures in the Gouveia and Oliveira (2008) experiment. Their cultures were grown in outdoor ponds that were subjected to fluctuations in temperature (Figure 17), whereas our cultures were temperature controlled. Furthermore, their experimental cultures received daily light dark cycles and changes in both light intensity and quality each day. The averaged peak biomass for the 15°C and 25°C cultures was 1.32 DW L⁻¹ which is comparable to 2.00 DW L⁻¹.

Table 13: Comparison to Gouveia and Oliveria (2008) results for *E. oleoabundans* for productivity and peak biomass.

Temperature °C	15			25			35			
Light Intensity $\mu\text{mol m}^{-2} \text{sec}^{-1}$	70	130	200	70	130	200	70	130	200	Gouveia and Oliveria (2008) outdoors
Productivity (gDW L ⁻¹ day ⁻¹)	1.37	1.43	1.28	1.71	1.16	0.88	0.06	0.05	0.02	0.09
Peak biomass (gDW L ⁻¹)	1.29	1.44	1.38	0.89	1.18	1.72	0.31	0.34	0.46	2.00

Gouveia *et al.* (2009) also analyzed oil production of *E. oleoabundans* growing in different amounts of nitrate. Growing at 30°C under 360 $\mu\text{mol m}^{-2} \text{sec}^{-1}$, in nitrogen starved conditions, the greatest peak percent oil per dry mass of algae was 56%, measured by Nile red fluorescence, which only measures total oil concentration, not concentration of individual lipids. Those cultures were also supplied with a 5% CO₂ enriched air mixture. In our experiment, the greatest peak percent oil per algae was obtained by cultures growing at 25°C under 200 $\mu\text{mol m}^{-2} \text{sec}^{-1}$, 56.7%. At 15°C under 130 $\mu\text{mol m}^{-2} \text{sec}^{-1}$, 55.93% was achieved. The peak percent oil per algae values at 15°C are all above 50% and at 25°C, the

values are above 40% (Table 14). Thus, our work is in agreement with the only other major study performed on *E. oleoabundans*.

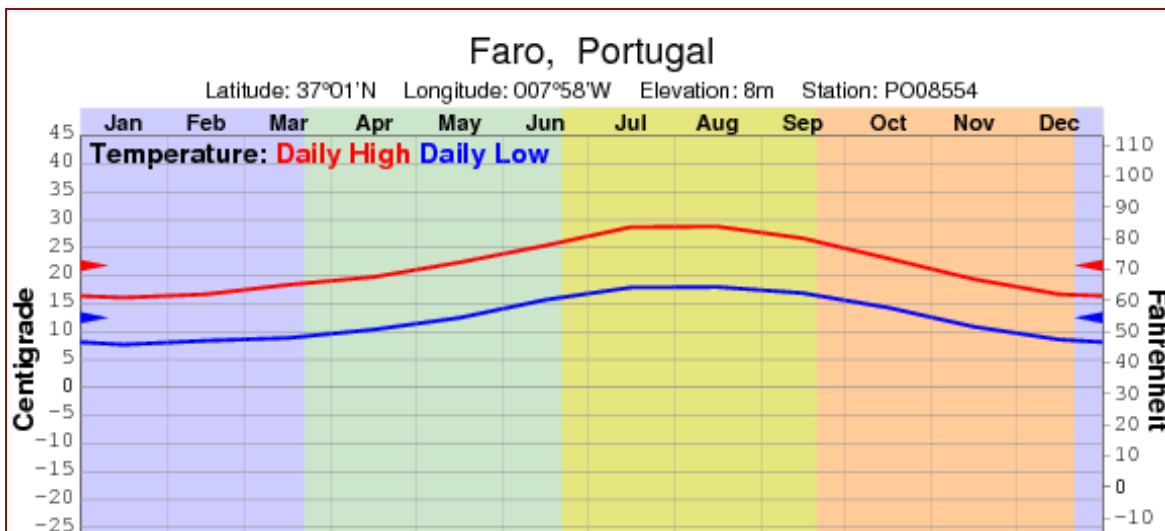


Figure 17: Average annual temperatures of Portugal (taken from Climate Charts, 2010).

Table 14: Comparison to Gouveia (2009) results for *E. oleoabundans* for peak oil per algae.

	Temperature (°C)									Gouveia <i>et al.</i> (2009) 30°C
	15			25			35			
Light Intensity (μmol/m ⁻² sec ⁻¹)	70	130	200	70	130	200	70	130	200	360
Peak %oil/algae	52.6	55.9	50.8	40.3	44.8	56.7	nd	nd	nd	56%

Although work done specifically with *E. oleoabundans* is sparse, there are some studies on the effect of these growth parameters on other algal species. For example, Sorokin and Krauss (1957) grew six different algae species, not including *E. oleoabundans*, under a wide range of light intensities ($0\text{--}21523 \mu\text{mol m}^{-2} \text{ sec}^{-1}$) and discovered that increasing the light intensity did not increase the growth rate of algal cultures. A statistical analysis of our data showed there was no significant difference in productivity, yield, and peak biomass between *E. oleoabundans* grown under 70, 130, and $200 \mu\text{mol m}^{-2} \text{ sec}^{-1}$. Therefore changing the light intensity between 70 and $200 \mu\text{mol m}^{-2} \text{ sec}^{-1}$ does not have any significant effect on *E. oleoabundans* growth. Rather, the major factor affecting growth in our study was temperature.

Cultures at 200 and $130 \mu\text{mol m}^{-2} \text{ sec}^{-1}$ in 35°C may have exhibited signs of chronic photoinhibition. Chronic photoinhibition occurs when photosynthetic organisms are exposed to high levels of light intensities for a long period time. Long exposure to high

intensities of light can damage the D Protein of Photosystem II, which causes a malfunction in the electron transport chain needed in photosynthesis to generate food for the organism. The D1 Protein is part of the photoinhibition repair cycle, but during prolonged exposure to high light intensities, the repair cycle is unable to fix and prevent damage to PSII (Han *et al.*, 2000). In the 35°C experimental run, it is possible that the D1 protein became denatured by the high heat. If this was the case, the D1 protein would not be able to prevent photo-oxidative damage from the continuous light at 200 $\mu\text{mol m}^{-2} \text{sec}^{-1}$ and 130 $\mu\text{mol m}^{-2} \text{sec}^{-1}$, resulting in photoinhibition of these cultures.

When Goldman and Carpenter (1974) performed a meta-study on the effects of temperature on algal growth, they created a model and determined that temperature can have an effect on algal growth, but it needs to be determined for each individual species. Our work represents an initial attempt to map the temperature growth relationship for *E. oleoabundans*. In another case, Eppley (1972) performed a study on saltwater phytoplankton growing at different temperatures and observed that there was an upper temperature limit for algal growth. All photosynthetic organisms have an optimal temperature response. As temperature increases, the rate of photosynthesis increases until the optimum temperature is reached. Once the temperature surpasses the optimal range, the rate of photosynthesis then begins to decline. This decline may be the result of damage to the enzyme Rubisco. If Rubisco, the first enzyme of the Calvin Cycle, was denatured by high heat, then the cultures would not have been able to fix CO₂. For most species, growth declined $\geq 40^\circ\text{C}$. For some species, however, the upper limit was even lower at 35°C.

Our work in addition to Gouveia and Oliveira (2008), indicates that the high temperature cut-off for *E. oleoabundans* is between 30 and 35°C. Bosma *et al.* (2007) posited that the effects of temperature on algal growth were a result of an impact on photosynthetic rates within the algae. They concluded that at sub-optimal temperatures, light absorbed by the photosystems could not be converted into carbohydrates because enzyme activity declined at low temperatures. Bernacchi *et al.* (2001) also demonstrated that Rubisco activity in leaf tissue is sensitive to high temperatures and this likely inactivates photosynthesis when the temperature is excessively high. Since Rubisco is vital to carbon dioxide fixation, damage to the enzyme is a likely cause of the decline in growth observed in our study when the algae were grown at 35°C.

There were many fluctuations in the growth curves of our cultures as noted in Section 4.1. *E. oleoabundans* reproduce by forming zoospores inside each cell, causing the mother cell to enlarge until it breaks open and releases the smaller zoospores (Yang, 2011). The process of cells enlarging and releasing the smaller new cells could be responsible for these fluctuations; however, correlation between microscopic analysis and cell size was not conclusive (data not shown). It has been hypothesized that *E. oleoabundans* may use the

lipids it produces as an energy source when the mother cells break open to release the zoospores (Yang et al., 2011).

The GC-MS analysis of the lipids extracted from the algae indicated that both temperature and light intensity affect oil composition. Although C18:1 was present in all of the samples, the amount of C18:1 varied between the conditions. Overall lipid composition and totals varied between conditions, with 25°C under 70 $\mu\text{mol m}^{-2} \text{sec}^{-1}$ the only condition to produce all three desired fatty acids for biodiesel production (C14:1, C16:1, and C18:1). At 15 and 25°C, there appeared to be a relationship between light intensity and double bond formation on the carbon skeleton of the lipids. At 200 $\mu\text{mol m}^{-2} \text{sec}^{-1}$ for both 15 and 25°C, the highest levels of C16:2, C16:3, C18:2, and C18:3 were observed, thus the highest light intensity produced more carbon double bonds. At 35°C, the 70 $\mu\text{mol m}^{-2} \text{sec}^{-1}$ cultures contained a similar, but not entirely the same composition of lipids to the healthier algae growing at 15 and 25 °C. The cultures growing under 35°C at 70 $\mu\text{mol m}^{-2} \text{sec}^{-1}$ also produced C14:0 and 16:1 with a ratio of 1.57:12.09:2.72, which still does not reach the ideal ratio of 5:4:1. Cultures growing at 35°C at 130 and 200 $\mu\text{mol m}^{-2} \text{sec}^{-1}$ produced a narrower lipid composition range than the other cultures. Although these cultures produced very low levels of lipids containing double bonds, the majority of the lipids were C16:0 and C18:0. The results and observation for 35°C further confirm that *E. oleoabundans* does not thrive at this high temperature. As discussed before, enzymes have optimal temperature ranges, and outside of those ranges function is diminished. If Rubisco was denatured by high heat, then the cultures would not have been able to fix CO₂ and provide the materials needed to make TAGs. Overall, these results are taken from an n=1, so the experiment must be replicated in order to draw stronger conclusions. and more research should focus on finding the conditions that produce a better ratio of the ideal biofuel fatty acids in *E. oleoabundans*.

Chapter 6: Conclusions and Future Research

Our results indicated that *E. oleoabundans* grows reasonably well at light intensities as low as 70 $\mu\text{mol m}^{-2} \text{sec}^{-1}$ without any negative effects to biomass productivity or yield, or to oil production. Furthermore, cultures grown at light intensities between 70 and 200 $\mu\text{mol m}^{-2} \text{sec}^{-1}$ did not demonstrate any significant variation in growth. Additionally, *E. oleoabundans* growth at 15 and 25°C was not significantly different. The higher temperature of 35°C appeared to be beyond the upper temperature limit for this species. This temperature is well above the annual average temperature range for the Northeastern, US. Thus, the ability to grow and produce oil in low light intensities and low temperatures indicate that *E. oleoabundans* would be a suitable algal species for producing biofuels in areas like New England.

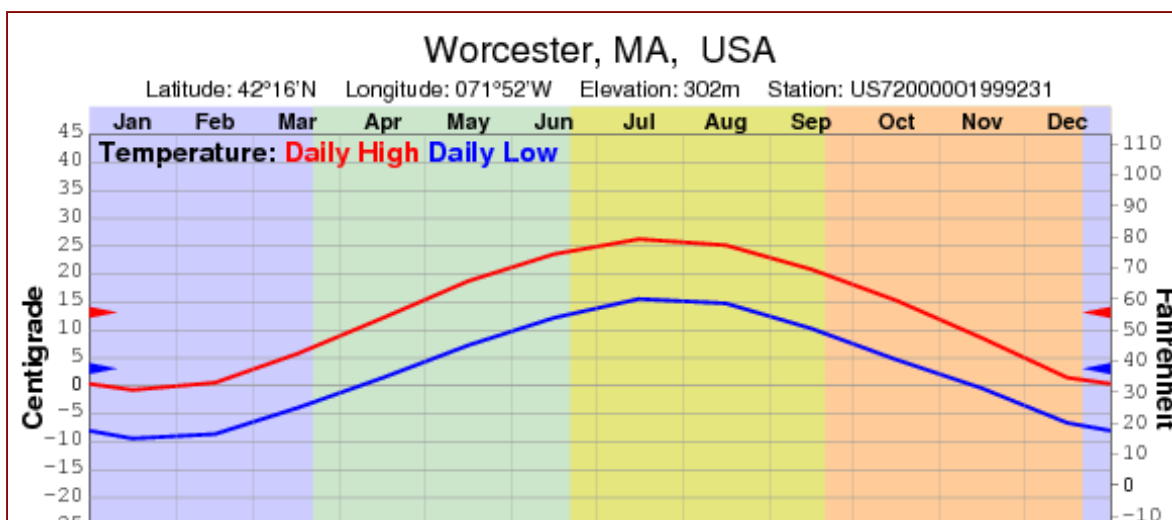


Figure 18: Average annual temperatures of Worcester, MA, a city in Northeastern US (taken from Climate-Charts, 2010).

Future research on *E. oleoabundans* should include more variables that may affect the optimization of growth and oil production conditions. Since CO₂ is vital for algal growth, the next project using this species should repeat our experiments, but with CO₂ supplementation. Moreover, our algae were also grown under continuous light and heat in the incubator, which differs from growing the algae in outdoor bioreactors. Algae cultures growing outside would be subjected to the effects of a day and night cycle and temperature fluctuations. It would be beneficial to video record *E. oleoabundans* under a microscope for a 24 hour period to obtain more basic lifecycle information on the species. To investigate the full potential of *E. oleoabundans* as an alternative and sustainable liquid transportation fuel, the effects of a day and night cycle and daily temperature variations on growth and oil production should be measured. Furthermore, future work should also focus on determining the nitrogen levels that result in the optimum growth and lipid production of *E. oleoabundans*. Also, since GC-MS analysis indicated that growth conditions have an effect on oil composition in the algae, it is important to determine the molecular relationship between light, temperature, growth and oil production in order to fully control *E. oleoabundans*. The end goal of all these future projects should be to optimize growing conditions *E. oleoabundans* in order to maximize growth and oil production, as well as produce the ideal mixture of fatty acids for biodiesel production. This project was only the beginning of the necessary journey to find a feasible and sustainable alternative liquid transportation fuel, thus it is important to continue research on *E. oleoabundans*.

References

- Apogee Instruments Inc. *Solar radiation questions.*, (2010), from http://www.apogeeinstruments.com/faq_solar.htm#Q3
- Bernacchi, E.J., Singaas, E.L., Pimentel, C., Portis Jr. A.R., Long, S.P., (2001). Improved temperature response functions for models of Rubisco-limited photosynthesis. *Plant, Cell and Environment*. 24(2), 253–259.
- Blankenship, R., (2002). *Molecular Mechanisms of Photosynthesis*. Oxford: Blackwell Science Ltd.
- Bosma, R., van Zessen, E., Reith, J., Tramper, J., Wijffels, R., (2006). Prediction of volumetric productivity of an outdoor photobioreactor. *Biotechnology and Bioengineering*, 97(5), 1108-1120.
- Campbell, W. and Ogren, W., (1992). Light Activation of Rubisco by Rubisco Activase and Thylakoid Membranes. *Plant and Cell Physiology*. 33 (6), 751-756.
- Carraretto, C., Major, A., Mirandola, A., Stoppato, A., Tonon, S., (2004). Biodiesel as alternative fuel: Experimental analysis and energetic evaluations. *Energy*, 29(12), 2195–2211.
- Chisti, Y., (2008). Biodiesel from microalgae beats bioethanol. *Trends in Biotechnology*, 26(3), 126-131.
- Climate-Charts, (2010). Climate Maps of Portugal and Worcester. <<http://climate-charts.com/>>.
- Darzins, A., Pienkos, P., Wolfrum, E., Ghirardi, M., (2008). *Algal biofuels technologies* National Bioenergy Center. <<http://www.nrel.gov/biomass/pdfs/49123.pdf>>.
- Day, J., Hall, C., Yanez-Arancibia, A., Pimental, D., Marti, C., Mitsch, W., (2009). Ecology in Times of Scarcity. *BioScience*, 59(4), 321-331.
- de Souza, S.P., Pacca, S., de Ávila, M. T., & Borges, J. L. B., (2010). Greenhouse gas emissions and energy balance of palm oil biofuel. *Renewable Energy*, 35(11), 2552-2561.
- Eppley, R.W., (1972). Temperature and Phytoplankton Growth in the Sea. *Fishery Bulletin*, 70(4), 1063-1085.

- Goldman, J.C., Carpenter, E.J., (1974). A kinetic approach to the effect of temperature on algal growth. *Limnology and Oceanography*, 19(5), 756-766.
- Gouveia, Luísa; Oliveira, A.C., (2008) Microalgae as a raw material for biofuels production. *J Ind Microbiol Biotechnol* 36(6),269-274.
- Gouveia, L., Marques, A., da Silva, T., Reis, A., (2009). *Neochloris oleoabundans* UTEX #1185: A suitable renewable lipid source for biofuel production. *Journal of Analytical and Applied Pyrolysis*, 36(6), 821-826.
- Grierson, S., Strezov, V., Ellem, G., McGregor, R., Herbertson, J., (2008). Thermal characterization of microalgae under slow pyrolysis conditions. *Journal of Analytical and Applied Pyrolysis*, 85(1), 118-123.
- Han, B., Virtanen, M., Koponen, J., Straškraba, M., (2000). Effect of photoinhibition on algal photosynthesis: a dynamic model. *Plankton Research*. 22(5), 865-885.
- Huang G., Feng, C., Wei, D., Zhang, X.W., Chen, G., (2009). Biodiesel production by microalgal biotechnology. *Applied Energy*, 87(1), 38-46.
- Kathiresan, S., Chandrashekar, A., Ravishankar, G.A, Sarada, R.,(2009). Agrobacterium-Mediated Transformation in the Green Alga *Haematococcus pluvialis* (Chlorophyceae, Volvocales) *J. Phycol.* 45(3), 642–649.
- Kim, Y., (2001). Assessment of Bioreactors for Transformed Cultures. Ph.D. thesis, Dept. Chemical Engineering, Worcester Polytechnic Institute, Worcester, MA.
- Kong, Q., Li, B., Martinez, B., Chen, P., Ruan, R., (2009). Culture of microalgae *Chlamydomonas reinhardtii* in wastewater for biomass feedstock production. *Applied Biochemistry and Biotechnology*, 160(1), 9-18.
- Knothe, G., (2005). Dependence of biodiesel fuel properties on the structure of fatty acid alkyl esters. *Fuel Processing Technology*. 86(10), 1059-1070.
- Li, Y., Markley, B., Mohan, A., Rodriguez-Santiago, V., Thompson, D., Van Niekerk, D., (2006). Utilization of carbon dioxide from coal-fired power plant for the production of value-added products. Pennsylvania State University. *Design Engineering of Energy and Geo-Environmental Systems*.
<http://www.ems.psu.edu/~elsworth/courses/egee580/Utilization_final_report.pdf>.

- Liaquat, A. M., Kalam, M. A., Masjuki, H. H., Jayed, M. H., (2010). Potential emissions reduction in road transport sector using biofuel in developing countries. *Atmospheric Environment*, 44(32), 3869-3877.
- Lung, S., and Weselake, R., (2006). Diacylglycerol Acyltransferase: A Key Mediator of Plant Triacylglycerol Synthesis. *Lipids*, 41(12), 1073-1088.
- Monash Scientific., (2000). Image of glycerol molecule. Dandenong, Australia.
<<http://www.monashscientific.com.au/GlycerolMolecule.htm>>.
- Mukhopadhyaya, K. and Forssell, O., (2005). An empirical investigation of air pollution from fossil fuel combustion and its impact on health in India during 1973–1974 to 1996–1997. *Ecological Economics*, 55(2), 235-250.
- National Aeronautics and Space Administration (NASA). (2010). *More on brightness as a function of distance*. <<http://imagine.gsfc.nasa.gov/YBA/M31-velocity/1overR2-more.html>>.
- National Biodiesel Board, (2010). Biodiesel Production. <<http://www.biodiesel.org/>>.
- Pachauri, N. and He, B., (2006). Value-added utilization of crude glycerol from biodiesel Production: a survey of current research activities. Biological and Agricultural Engineering at the University of Idaho.
<http://www.webpages.uidaho.edu/~bhe/pdfs/asabe066223.pdf>
- Qin, J., (2005). Bio - hydrocarbons from algae *Australian Government*, 25(5), 26.
<<https://rirdc.infoservices.com.au/downloads/05-025.pdf>>.
- Rasmussen, M., (2008). *Carbon dioxide capture with algae* (Power Point Presentation ed.) SarTech. <<http://www.sartec.com/co2capture.pdf>>.
- Rutz, D., & Janssen, R. (2007). Biofuel technology handbook.
<http://www.co2star.eu/publications/BioFuel_Technology_Handbook_1vs_WIP.pdf>.
- Schenk, P., Thomas-Hall, S., Stephens, E., Marx, U., Mussgnug, J. Posten, C., Kruse, O., Hankamer, B., (2008). Second Generation Biofuels: High-Efficiency Microalgae for Biodiesel Production. *Bioengineering Resource*. 1(1), 20-43.
- Schober, S., Mittelbach, M., (2007). Iodine value and biodiesel: Is limitation still appropriate? *Lipid Technology*, 12(19), 281-284.

- Scragg, A. H., Morrison, J., Shales, S.W., (2001). The use of a fuel containing *Chlorella vulgaris* in a diesel engine. *Enzyme and Microbial Technology*, 33(7), 884-889.
- Senauer, B., (2008). Food market effects of a global resource shift toward bioenergy. *American Journal of Agricultural Economics*, 90(5), 1226-1232.
- Solovchenko, A.E., Khozin-Goldberg, I., Didi-Cohen, S., Cohen, Z., Merzlyak., (2007). Effects of light intensity and nitrogen starvation on growth, total fatty acids and arachidonic acid in the green microalga *Parietochloris incise*. *Journal of Applied Phycology*, 20(3), 245-251.
- Sorokin, C. and Krauss, R. (1957) The effects of light intensity on the growth rates of green algae. *Plant Physiology*, 33(2), 109-113.
- Taiz, L., Zeiger, E., (2010). *Plant Physiology Fifth Edition*. Sinauer Associates. Sunderland, MA. Chapter 9.
- Towler, M., (2005). Effects of inoculum density, carbon concentration, and feeding source on the growth of transformed roots of *Artemisia annua* in a modified nutrient mist bioreactor. Ph.D. thesis, Dept. Biology and Biotechnology, Worcester Polytechnic Institute, Worcester, MA.
- Van Baalen, C., Hoare, D., Brandt, E., (1970). Heterotrophic growth of blue-green algae in dim light. *Journal of Bacteriology* 105(3), 685-689.
- Wahal, S., and Viamajala, S., (2010). Maximizing algal growth in batch reactors using sequential change in light intensity. *Applied Biochemistry and Biotechnology*, 161(1), 511-522.
- Wright, J., (2008). Oil: Demand, supply and trends in the United States. University of California Berkeley.
http://dr.berkeley.edu/pdfs_to_post/OIL_OVERVIEW_OF_5DECADE_HISTORY_AND_TODAYS_CHALLENGES-1.pdf
- Yang, Y., Xu, J., Vail, D., Weathers, P., (2011). *Ettlia oleoabundans* growth and oil production on agricultural anaerobic waste effluents. *Bioresource Technology*, 102(8), 5076-5082.

Appendix A

Bold's Basal Media (BBM)

To prepare the final medium, begin with 700-800mL of dH₂O and add 10 mL of the first six stock solutions. Add 1 mL each of the alkaline EDTA, acidified iron, boron and trace metals solutions. Autoclave. The final pH should be 6.4, adjusted using NaOH and KMNO₄.

Component	400 mL Stock Solution	1 Liter Stock Solution	add quantity below per liter of medium	Molar Concentration in Final Medium
Major Stock				
NaNO ₃	10 g L ⁻¹ dH ₂ O	25.00 g L ⁻¹ dH ₂ O	10 mL	2.94 x 10 ⁻³ M
CaCl ₂ • 2H ₂ O	1 g L ⁻¹ dH ₂ O	2.50 g L ⁻¹ dH ₂ O	10 mL	1.70 x 10 ⁻⁴ M
MgSO ₄ • 7H ₂ O	3 g L ⁻¹ dH ₂ O	7.50 g L ⁻¹ dH ₂ O	10 mL	3.04 x 10 ⁻⁴ M
K ₂ HPO ₄	3 g L ⁻¹ dH ₂ O	7.50 g L ⁻¹ dH ₂ O	10 mL	4.31 x 10 ⁻⁴ M
KH ₂ PO ₄	7 g L ⁻¹ dH ₂ O	17.50 g L ⁻¹ dH ₂ O	10 mL	1.29 x 10 ⁻³ M
NaCl	1 g L ⁻¹ dH ₂ O	2.50 g L ⁻¹ dH ₂ O	10 mL	4.28 x 10 ⁻⁴ M
<u>Alkaline EDTA Stock Solution</u>			add 1 mL of this solution per liter of medium	
EDTA anhydrous		50 g L ⁻¹ dH ₂ O		4.28 x 10 ⁻⁴ M
KOH		31 g L ⁻¹ dH ₂ O		1.38 x 10 ⁻³ M
<u>Acidified Iron Stock Solution</u>			add 1 mL of this solution per liter of medium	
FeSO ₄ • 7H ₂ O		4.98 g L ⁻¹ dH ₂ O		4.48 x 10 ⁻⁵ M
H ₂ SO ₄		1.0 mL		
<u>Boron Stock Solution</u>			add 1 mL of this solution per liter of medium	
H ₃ BO ₃		11.42 g L ⁻¹ dH ₂ O		4.62 x 10 ⁻⁴ M
<u>Trace Metal Stock Solution</u>			add 1 mL of this solution per liter of medium	
ZnSO ₄ • 7H ₂ O		8.82 g L ⁻¹ dH ₂ O		7.67 x 10 ⁻⁵ M
MnCl ₂ • 4H ₂ O		1.44 g L ⁻¹ dH ₂ O		1.82 x 10 ⁻⁵ M
MoO ₃		0.71 g L ⁻¹ dH ₂ O		1.23 x 10 ⁻⁵ M
CuSO ₄ • 5H ₂ O		1.57 g L ⁻¹ dH ₂ O		1.57 x 10 ⁻⁵ M
Co(NO ₃) ₂ • 6H ₂ O		0.49 g L ⁻¹ dH ₂ O		4.21 x 10 ⁻⁶ M

Bold, H.C. 1949. The morphology of *Chlamydomonas chlamydogama* sp. nov. *Bull. Torrey Bot. Club.* **76**: 101-8.

Bischoff, H.W. and Bold, H.C. 1963. Phycological Studies IV. Some soil algae from Enchanted Rock and related algal species. Univ. Texas Publ. 6318: 1-95.

Appendix B

15 Watt GE Kitchen & Bath Starcoat® T8

PRODUCT INFORMATION

ANSI Code	2009-1
Base	Medium Bi-Pin (G13)
Product Code	21326
Description	F15T8/KB 6PK
UPC	43168980692

GENERAL CHARACTERISTICS

Lamp type	Linear Fluorescent - Straight Linear
Bulb	T8
Base	Medium Bi-Pin (G13)
Wattage	15
Voltage	55
Rated Life	7500 hrs
Bulb Material	Soda lime
Starting Temperature (MIN)	10 °C (50 °F)
Primary Application	Kitchen & Bath

PHOTOMETRIC CHARACTERISTICS

Initial Lumens	940
Mean Lumens	850
Nominal Initial Lumens per Watt	62
Color Temperature	3000 K
Color Rendering Index (CRI)	70

ELECTRICAL CHARACTERISTICS

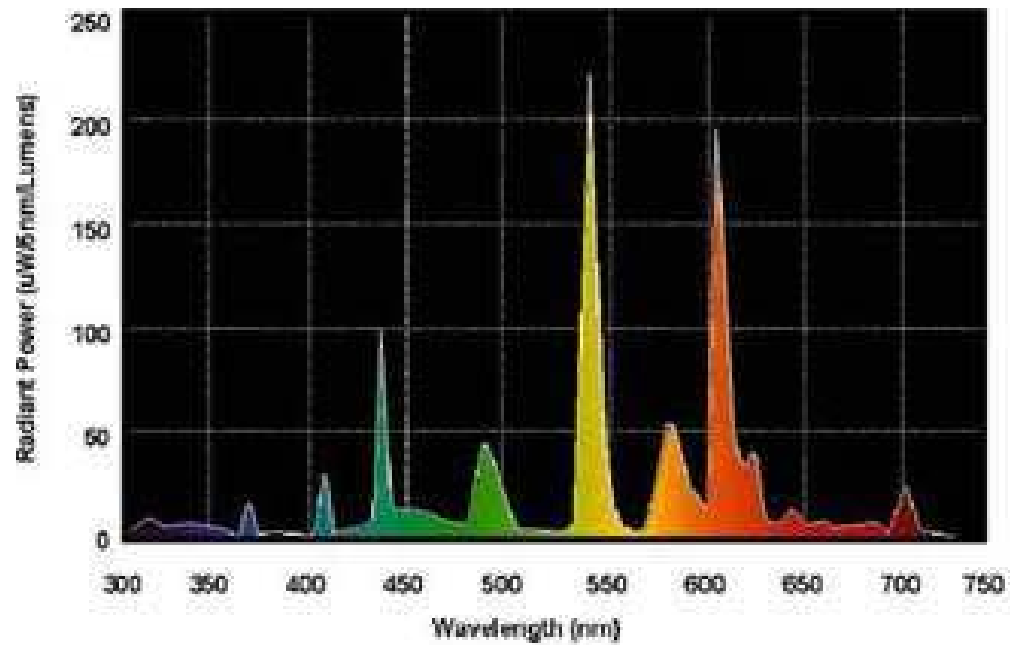
Open Circuit Voltage (rapid start) (MAX)	220 V
Open Circuit Voltage (after preheating) Max @ Temperature	210 V @ 10 °C
Open Circuit Voltage (rapid start) Min @ Temperature	157 V @ 10 °C
Cathode Resistance Ratio - Rh/Rc (MIN)	4.25
Cathode Resistance Ratio - Rh/Rc (MAX)	6.5
Open Circuit Voltage (after preheating) Min @ Temperature	108 V @ 10 °C
Current Crest Factor (MAX)	1.7

DIMENSIONS

Maximum Overall Length (MOL)	17.7800 in (451.6 mm)
Minimum Overall Length	17.6700 in (448.8 mm)
Nominal Length	18.000 in (457.2 mm)
Bulb Diameter (DIA)	1.000 in (25.4 mm)
Bulb Diameter (DIA) (MIN)	0.940 in (23.8 mm)
Bulb Diameter (DIA) (MAX)	1.100 in (27.9 mm)
Max Base Face to Base Face (A)	17.220 in (437.3 mm)
Face to End of Opposing Pin (B) (MIN)	17.400 in (441.9 mm)
Face to End of Opposing Pin (B) (MAX)	17.500 in (444.5 mm)
End of Base Pin to End of Opposite Pin End (C)	17.670 in (448.8 mm)

Appendix B Continued

15 Watt GE Kitchen & Bath Starcoat® T8 Spectral Power Distribution Curve



Appendix C

Procedures for Nile Red Lipid Assay (from Yang, personal communication)

1. Load the well (in 96-well plate) with 5 μ l algal cell suspensions and then 3 μ l 50 μ g/ml Nile Red DMSO solution;
2. The corresponding sample blank is prepared by loading another cell with 5 μ l algal cell suspensions alone without Nile Red staining;
3. Add 292 μ l DMSO aqueous solution (25% v/v) to each of the well (cells with or without staining);
4. Place the 96-well plate (with lid on) on a shaker at 100 rpm for 10 min;
5. After shaking, transfer the plate (with lid on) to a 37 $^{\circ}$ C incubator for 10 min (color development should be complete by the end of incubation);
6. Put the plate into the Wallac 1420 multilabel counter for fluorometry assay.

Log in, click the Wallac 1420 program on the desktop, select the appropriate protocol 'Nile Red Lipid', click the button 'define platemap and start run using Wallac 1420 starting wizard'

Next \rightarrow Wobbe Lab \rightarrow highlight 'Nile Red Lipid' \rightarrow Next \rightarrow define platemap \rightarrow Next \rightarrow start the run

During the assay, may click 'Live display' to view the relative fluorescence emission simultaneously.

At the end of the assay, click the button 'Latest assay run'

File \rightarrow Export \rightarrow Choose or create a folder to save the data in Excel.

Finally, close the 'Wallac 1420 Manager'.

The relative fluorescence (in arbitrary unit) is calculated by subtracting the reading of algal culture blank from that of the corresponding stained cell. Samples are always prepared in triplicate.

Appendix D

Procedures for lipid gravimetric determination (from Yang, personal communication)

1. Twenty-milliliter of the algal culture was harvested by centrifugation at 7500 rpm for 15 min;
2. After centrifugation, the wet pellets were re-suspended in 15 ml phosphate buffer* (pH = 7.4, 50 mM) to minimize side reaction during cell destruction;
3. The re-suspended algal cells were destructed by a bead-beater (Biospec, Model HBB908) for 1 min using 1 mm glass beads;
4. The slurry, together with the beads, were transferred to a centrifugation tube and centrifuged at 5000 rpm for 10 min;
5. After centrifugation, the slurry was removed to a test tube and mixed with 12 ml chloroform:methanol (2:1, v/v) solvent;
6. The aqueous-organic bi-phase mixture was shaken vigorously for 20 min, transferred to a separation funnel, and let stand for 30 min for complete separation of the two phases;
7. The bottom layer (organic) was collected and the top layer (aqueous) was extracted again following steps 5 & 6;
8. Two organic layers collected separately were combined, 20 ml 5% (w/v) NaCl solution was added to the organic phase and the new bi-phase system was shaken for washing purposes;
9. The bottom layer (organic) was collected in a test tube and evaporated to dryness by a nitrogen evaporator (Organomation Associates, Inc., Model N-EVAP™ 111).
10. The dry extractives remained at the bottom of the test tube was re-dissolved by adding 1 ml of the chloroform:methanol (2:1, v/v) solvent and the 1 ml solution was transferred to a pre-dried and pre-weighed aluminum weighing plate (2 ml HPLC amber vial???). Upon the completion of evaporation in the fume hood, the plate was moved to a 60 °C oven, dried for 1 h, and finally to a desiccator for 2 h.
11. The plate was weighed and put back to the desiccator again for another 2-h drying till constant weight was achieved. Constant weight was defined as less than 0.3 mg change in two successive weighings.

Weight of lipid = Weight of (aluminum plate + lipid) - Weight of aluminum plate

*Preparation of phosphate buffer

(<http://www.egr.msu.edu/biofuelcell/tools/phosphate/phosphate.html>):

1.5584 g/L NaH₂PO₄·H₂O

10.3736 g/L Na₂HPO₄·7H₂O ~ 5.4965g/L Na₂HPO₄ → pH 7.4, buffer strength 50 mM

Appendix E

Procedures for nitrate analysis (from Kim, 2001)

Szechrome NAS reagent preparation 0.5%

0.5g of Szechrome NAS (Polysciences, Inc. cat. No. 08762-5g) dissolve in 50:50 mL of Orthophosphoric acid (H_3PO_4) [Fluka 79617-1L] : Sulfuric acid 95-98% (H_2SO_4) [sigma 320501-2.5L] total 100mL i.e., 0.5% w/v.

Sample preparation:

My MS medium contains 7.7 mM (612 mg/L) of NH_4NO_3 and 15.15 mM (1.532 g/L) of KNO_3 , which have total 1.414 g/L of NO_3 (i.e., 78% of NO_3 (0.474 mg) is coming from NH_4NO_3 and 61% of NO_3 (0.940 mg) is coming from KNO_3)

To prepare my samples I used the following procedure

For control I took 1 uL of autoclaved medium (without root inoculation) and add 249 uL of HPLC grad water (final volume 250 uL): all other culture samples I took 10 uL and add 240 uL of HPLC grad water (final volume 250 uL) and then each sample add 2.5 mL of 0.5% Szechrome NAS reagent mix thoroughly and leave in room temperature for 45 min and then measure OD and 570nm.

Calculation = concentration value x 1000

1 for control

10 for sample

Appendix F

Procedures for phosphate analysis (from Towler, M.)

Phosphate reagent preparation:

Solution A: 9.44 mL of H_2SO_4 dissolve in 108.5 mL of dis H_2O , Then dissolve 0.472 g of ammonium molybdate (sigma A7302-100G) and make up 118 mL with above said solution (i.e. 108.5 mL H_2SO_4 with water).

Solution B: 2.36 g PVP (sigma P2307-500G) dissolve in 118 mL of dis H_2O .

Then mix solution A and B, then add 0.96 g of Ferrous ammonium sulfate $(\text{NH}_4)_2\text{Fe}(\text{SO}_4)_2 \times 6\text{H}_2\text{O}$ [sigma F1543-500G].

Sample preparation:

My MS medium 1L contains 170 mg of KH_2PO_4 which have 69.8% of PO_4 i.e. 118.66 mg/L.

To prepare sample I used following procedure

Fpr al culture samples I tool 20 uL and add 30 uL of HPLC grad water (final volume 50 uL) and then each sample add 1.5 mL of phosphate reagent mix thoroughly and leave in room temperature for 10 min and then measure OD and 650nm.

Calculation= concentration value x 1000

20 for sample